# Chapter 3: *Hox* Network

It turns out to be remarkably difficult for mathematicians and computer scientists who are enthusiastic about biology to learn enough biology not to be dangerous, and vice versa. After all, many of us became biologists because we didn't like math. For biologists to learn the mathematics turns out to be challenging in quite a different way. And there is a huge amount of non-understanding—I would not go so far as to say misunderstanding—that results. But getting these disciplines together has turned out to be a much easier thing to say than to do…We have to do a much better job of teaching at the interfaces of the disciplines.

- David Botstein, 2002

## *Introduction*

The problem under investigation is a study of the *Hox* regulatory mechanism in the developing hindbrain using a mathematical model based on a stochastic simulation algorithm (SSA) presented in Chapter 2. Much of this chapter is based on my paper published in the journal *Developmental Biology* (Kastner et al., 2002).

## *Developmental Biology Introduction*

In developmental biology, the establishment of asymmetry early in embryogenesis sets the stage for the formation of the body proper. The first axis formed

is along the anterior-posterior (or rostral-caudal) axis of the embryo. Cells are endowed with positional information that allows the proper formation of structures that correspond to their position along the axis. In other words, head structures form from the anterior part of the newly formed axis, and tail structures form from the posterior part of the axis.

The beginnings of the central nervous system in vertebrates occur early in development with the formation of the neural plate. The neural plate then folds into the neural tube. There are variations in how this occurs in different species, but in general the process is fairly similar: the tube begins as a groove down the midline of an embryo, and eventually closes from the joining of the flaps on either side (Gallera, 1971). This is a crucial process in development, and if the neural tube fails to close properly it can lead to defects like Spina bifida or Anencephaly (Van Allen et al., 1993).

Although initially straight, the upper section of the neural tube nearest the head forms a variety of bulges and constrictions that compartmentalize brain and spinal cord into distinct sections. The anterior most bulges will give rise to cells that make the prosencephalon (forebrain) and structures such as the olfactory lobes, the cerebrum, and the retina. Just posterior to that, the mesencephalon (midbrain) will give rise to structures like the optic lobes and the tectum. The most posterior bulges are the developing rhombencephalon (hindbrain) which gives rise to the cerebellum and the brain stem (Gilbert, 1997). Shortly after the closure of the neural tube, the vertebrate hindbrain further develops a series of axial bulges called rhombomeres that effectively compartmentalize the rhombencephalon into 8 smaller segments. The rhombomeres have been shown to be cell lineage restricted in that cells from one rhombomere do not cross over into another (Fraser et al., 1990). The segmentation of the hindbrain into

rhombomeres is a crucial process in the proper specification of the developing structures

of the hindbrain (Guthrie and Lumsden, 1991). In a series of closely aged chick embryos,

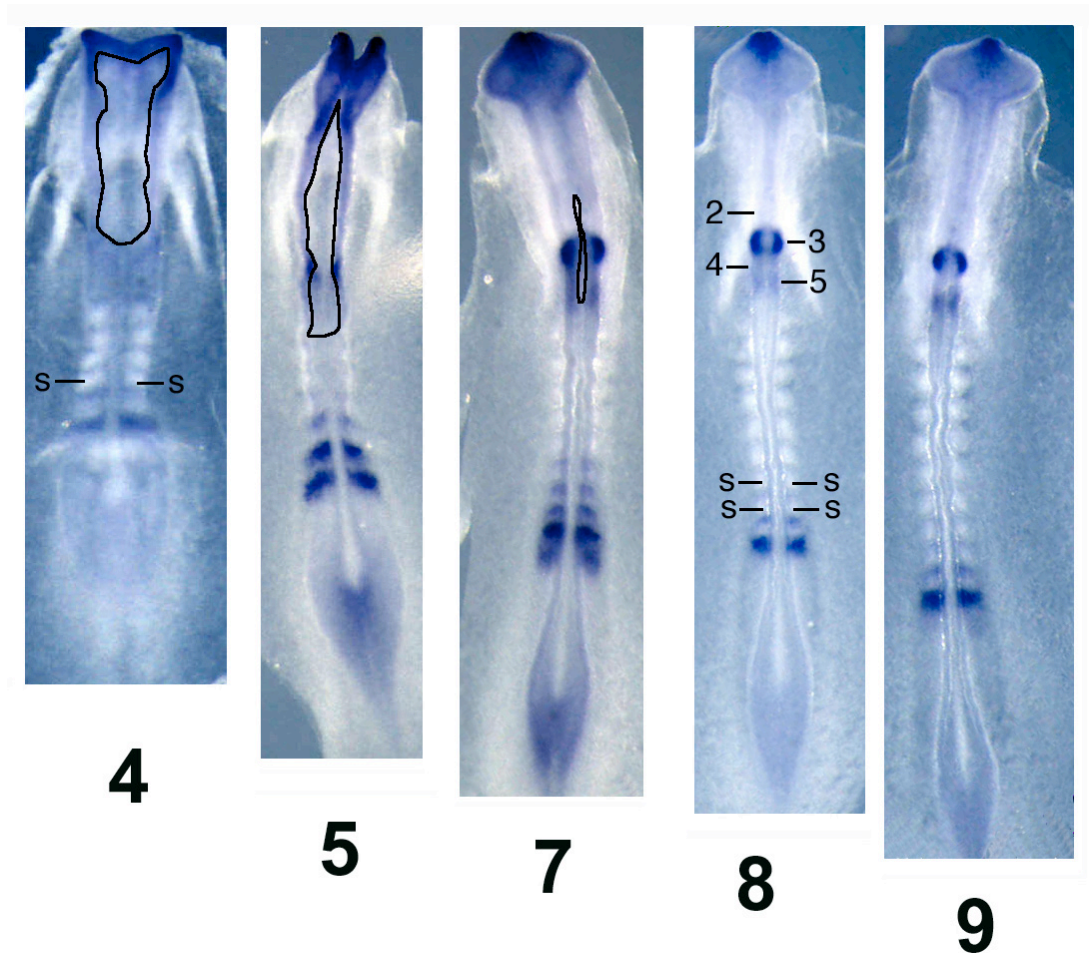Figure 3.1 shows the closing of the neural tube and the rhombomeres.



**Figure 3.1 Neural tube closure and rhombomere emergence**. These five embryos

are stained for the segmentally expressed gene *EphA4* (previously called *Sek2*, the

probe is courtesy of C. Tabin). The embryos are oriented with the head at the top of

the page and the tail at the bottom. The somites (examples marked by **S** in **4** and **8**

above) are block-like collections of cells that form in pairs along the rostral-caudal

axis of the embryo. They appear in a regular fashion, a new pair appearing every 90

minutes or so.  Because of this, the somites are commonly used for a staging

mechanism and the numbers below the embryos are the pairs of somites in each

embryo.  The outlined areas in **4**, **5** and **7** show the gap between the neural folds

before the neural tube is fully closed in the mid and hindbrain.  Notice that in **4** the

tube is wide open, in **7** the tube is almost completely closed, and in **8** and **9** the tube is

closed.  In **8** rhombomeres 2 through 5 are marked, with rhombomere 3 being the

most prominent due to its strong expression of *EphA4*.  Rhombomere 3 is also clearly

visible in **7**.  A slightly different version of this figure will be appearing in the 7$^{th}$

edition of the book Developmental Biology by S. Gilbert.


The rhombomeres are transitory structures that appear for about 15% of the

development time of the embryo.  In the chick, they appear after about 25 hours of

development, and disappear by the100 hour mark.  In a cartoon adapted from Lumsden

(1990), Figure 3.2 shows the order and approximate timing of the formation of

rhombomere boundaries.  The *Hox* gene network under investigation is expressed in
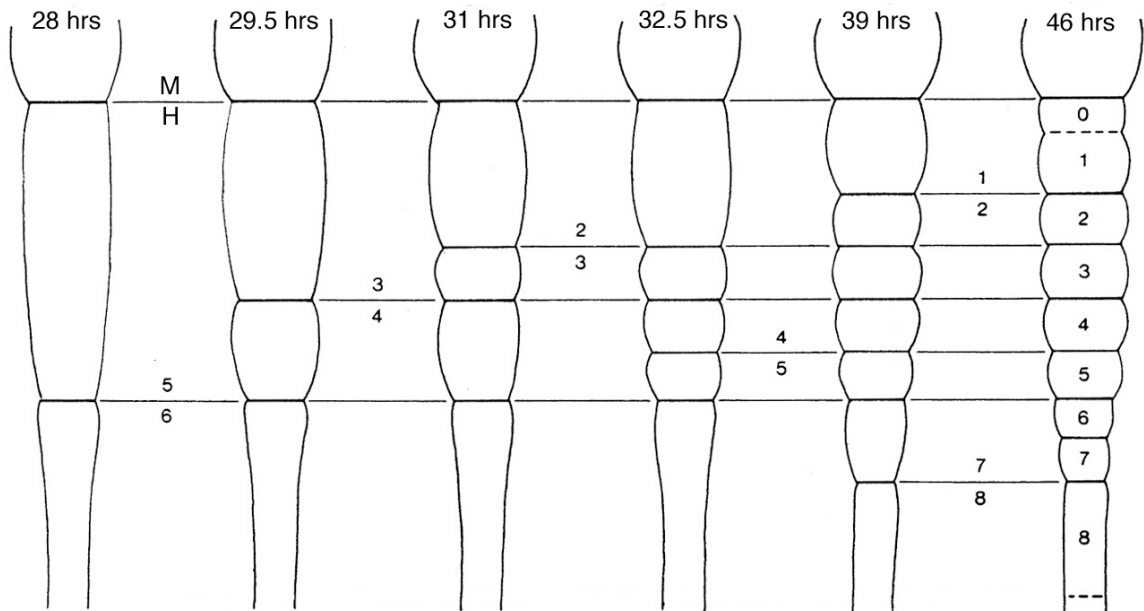
rhombomeres 4 and 5.

**Figure 3.2 Rhombomere emergence**. The first boundaries noticeable are the boundary between the midbrain and hindbrain (M/H), and the boundary between rhombomeres 5 and 6 (r5 and r6), both visible by 28 hours of development. The first fully formed rhombomere is r3 at 31 hours of development, followed by r4 and r5 at 32.5 hours, r2 at 39 hours, then r6, r7, r8 and r1 by 46 hours. The existence of rhombomere 0 is under debate, and there is no discernable boundary between rhombomere 8 and the developing spinal cord. The initial formation of the 5/6 boundary is actually very dependent on incubation conditions, and the initial start time may vary significantly.

## Introduction to the Control and Expression of Genes

This section contains a short introduction to the molecular biology behind the control and expression of genes. It is not intended to be all encompassing, and for more details, the reader is directed to Alberts et al. (1994). However, it is intended to give the reader enough information to follow the construction of the model presented below.

The problem of tissue differentiation mentioned above also needs to be addressed at a different level: that of the cell. The different cells in a multicellular organism contain the same DNA yet they differentiate from each other by creating and accumulating different messenger RNA (mRNA) and different proteins. The process by which a cell creates protein can be broken down into two major pieces: transcription and translation.

Transcription is the process by which mRNA is created from the DNA, while translation is the process by which the mRNA is turned into protein. Collectively, this process is called the Central Dogma. Obviously this is a simplified view as many other steps can occur. These include RNA splicing in which parts of the RNA are excised from the original strand. But while these steps are important in understanding the biology of the problem, they are not crucial to include from a modeling standpoint. This is because each of these steps is part of a cascade that affects the timing of the end result, but not what the end result is.

Transcriptional activators are the major building blocks of the model and it is this process that garners the most attention. Transcriptional factors are proteins that recognize a defined DNA sequence in the regulatory control region of a particular gene. Factors can be activators, which means that they contribute to the making of mRNA, or

repressors that prevent the mRNA for that gene being made. When even one molecule of a transcription factor is available for binding to the regulatory region of a gene, the probability that transcriptional will occur is significantly increased. Transcriptional control is a very complicated process and it can take multiple transcription factors acting in tandem to switch the gene on and allow the transcription of mRNA. This work focuses on the *cis*-regulation of genes: regulation that is controlled by sequences close to the start site for transcription. *Cis*-regulatory factors are generally the most important elements in transcription initiation.

## *Hox* Genes

Discovering regulatory genes, genes that control the major aspects of a biological system, has been the focus of biological research ever since molecular tools have become available. While no single master regulator gene has appeared, there have been some remarkable discoveries in developmental biology in the past few decades. In particular the homeotic genes have been identified as a family of genes that control genetic aspects of development (Duboule, 1994). First identified in the fruit fly *Drosophila melanogaster,* an evolutionary study showed that the homeobox—a set of 60 amino acids found in several different genes in *Drosophila* and encoding a DNA binding domain—also appeared in beetles, earthworms, chicken, mouse, and human (McGinnis et al., 1984). Mutation studies have been carried out in *Drosophila*, and they show that if a homeobox gene is mutated, the axial organization of the body is altered, leading researches to conclude that the homeobox genes are critical in the proper formation of the body plan (McGinnis and Krumlauf, 1992). In addition, it now appears that the

homeobox genes might indeed be the master regulatory genes of the body axis. It has recently been shown that natural alterations in the homeobox protein Ubx are likely to be the critical event that led to the evolution of hexapod insects from multilegged crustacean ancestors (Ronshaugen, 2002).

The 39 *Hox* (homeobox containing) genes found in higher vertebrates—like human and mouse—are organized into four chromosomal clusters located on different chromosomes. A *Hox* related family is found in invertebrates as well, but in this instance the genes can be found in a single cluster on one chromosome. Using information about their amino acid makeup, the genes can be aligned to one another using the *Drosophila* genes as a reference. They are easily grouped into13 paralog groups, or subfamilies. The *Hox* genes are collinear: the order they appear on the chromosome is the same as the order in which they appear in the body axis. Not only that, they have a temporal expression that is related to the order on the chromosome as well; the lower numbered families appear earlier in development than the higher number families. Finally, they also have a response to retinoic acid (RA), both in sensitivity and in the efficiency of the binding, that can be correlated to their order on the chromosome; the lower number families are very sensitive to RA and bind it tightly (when there is a retinoic acid response element in the control region of the gene), and the higher numbered families are less sensitive to RA and bind it more weakly. This information is summarized graphically in Figure 3.3 below.
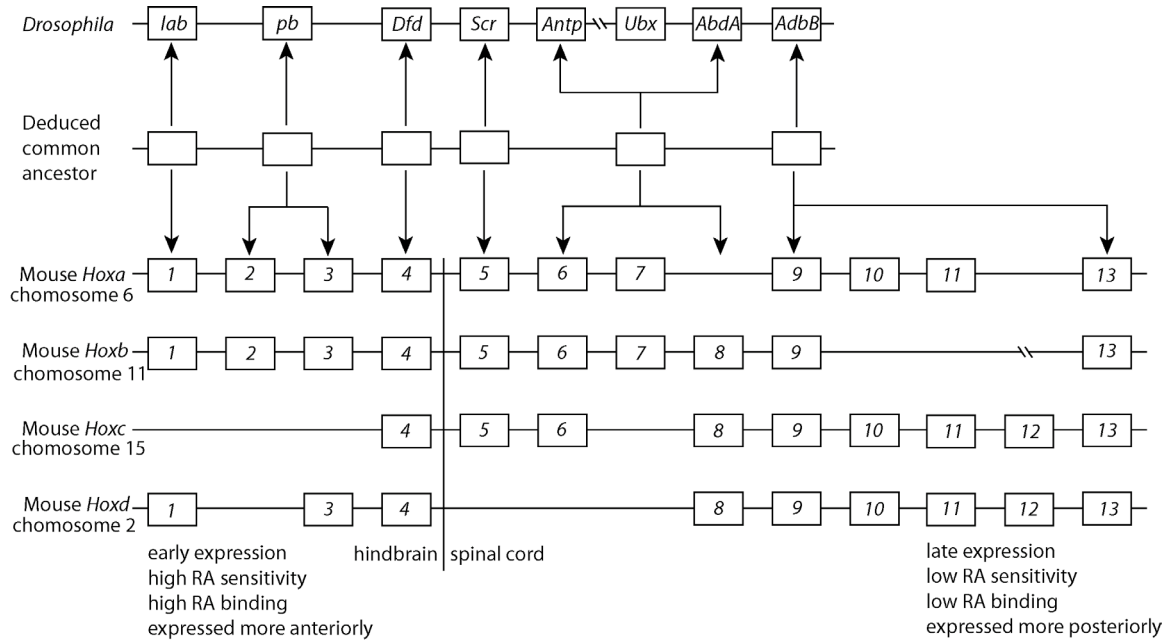
**Figure 3.3 Hox Paralog families** Alignment of the *Drosophila* HOM-C complex, the four mouse *Hox* chromosomal clusters, and their deduced common ancestor. After (Lufkin, 1997), with additional information from (Neuteboom and Murre, 1997; Pellerin et al., 1994).

The *Hox* gene family is a set of transcription factors that has been shown to be crucial in helping to confer rhombomere identity (Wilkinson, 1993). This can be shown dramatically by altering the expression of just a single gene: it was shown that misexpression of *Hoxb1* was able to transform rhombomere identity (Bell et al., 1999). The *Hox* genes exhibit rhombomere-restricted patterns of expression and the expression of several major rhombomere restricted genes (including the *Hox* genes) is shown below in Figure 3.4A.

But Figure 3.4A is very idealized. While the *Hox* genes certainly display rhombomere restricted patterns of expression, the expression does not stop cleanly at the boundaries.  This is best shown in Figures 3.3B, a 10x magnification picture of rhombomeres 3 through 7 (r3-r7) of a chick embryo stained for *Hoxb1*.
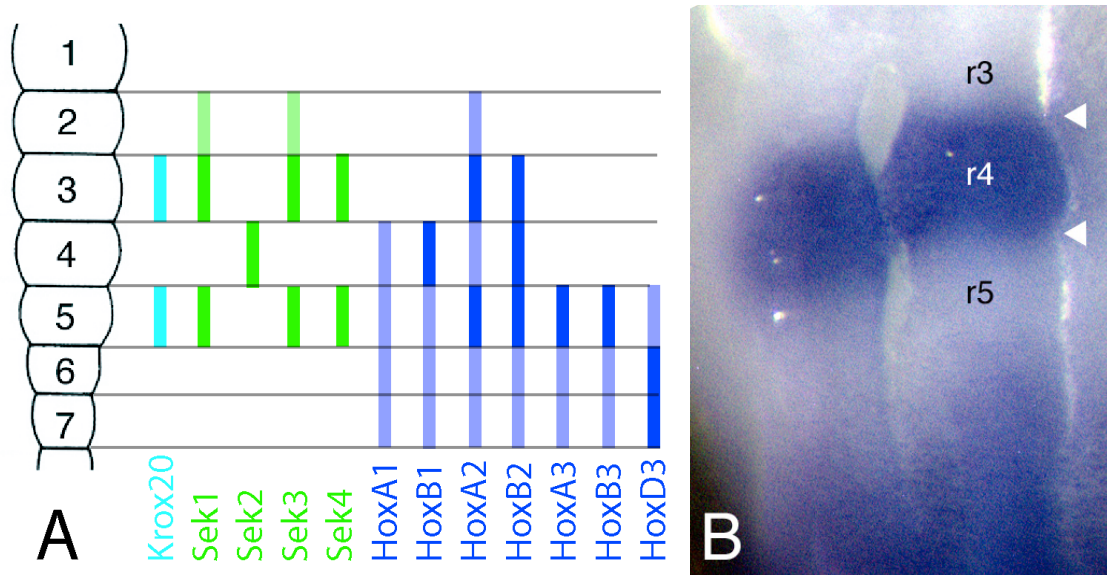


**Figure 3.4 Rhombomere restricted expression of several genes** **(A)** Expression patterns for several genes with rhombomere restricted boundaries. The lighter colors signify transient expression, and the darker colors correspond to continued levels of expression.  After (Lumsden and Krumlauf, 1996). **(B)** A10x picture of r3 (top) through r7 (bottom) of a chick hindbrain that has been stained for the gene *Hoxb1* (probe courtesy of R. Krumlauf).  The rostral and caudal boundaries of r4, as exemplified by the bulge in the tissue, have been marked with arrows. Notice that the gene expression is essentially restricted to r4, but the boundary is not a sharp one and there is some expression of the gene in the adjacent rhombomeres, most notably r3.

## Retinoic Acid

It has been long known that elevated levels of the retinoid vitamin A disturbs axial formation in vertebrates (Kalter and Warkany, 1959) and recently it has been shown that sufficient levels are necessary for proper development (Niederreither et al., 1999). Retinoic acid (RA) is the biological active derivative of vitamin A, and it acts through two classes of receptors, the RA receptors (RAR) $\alpha$, $\beta$, and $\gamma$ and the retinoid X receptors (RXR) $\alpha$, $\beta$, and $\gamma$. RA also plays an important part in the this process as it is able to directly regulate the expression of *Hox* family members, and alterations in the RA response elements in the *cis*-regulatory domain of reporter genes significantly change the expression patterns (Gavalas and Krumlauf, 2000).

## *Modeling*

## Network Creation

Stochastic investigations in biology models have so far been focused on intracellular systems. The goal of this thesis was to explore the utility of a SSA approach to modeling a gene network involving many cells. The direct coupling of the SSA implementation of a network and individual molecular events would seem to lend itself to both the analysis and logical organization of the ever growing data on the control of *Hox* genes in the developing hindbrain. The analysis presented here shows that the approach captures the timing, patterning, and variation in *Hox* gene expression without the need for artificially injected noise. The tests against some of the available experimental

perturbations suggest that the SSA will have predictive value and allow researchers in the laboratory to identify and focus attention on the most fruitful experiments.

Several of these predictions are noted, and two experiments were designed to clarify and test aspects of the model. One of the experiments (found in Chapter 4) suggested that a design decision made during the creation of the model was incorrect. The novel biological data resulted in a refinement of the model, thus closing the loop between modeling and experiments.

The SSA investigation into the *Hox* network focused on an investigation of the interaction of *Hoxa1*, *Hoxb1*, *Hoxb2*, *Krox20* and RA in rhombomeres 4 and 5 (r4 and r5). *Krox20* is not a homeobox gene, but it regulates *Hox* genes and is important for proper segmentation (Schneider-Maunoury et al., 1993). As mentioned previously, this system was chosen for a variety of reasons including the amount of information that is known: the molecular studies of the hindbrain have offered sufficient details to assemble a model for the interactions important in regional control of gene expression. In addition, the accessibility of the chick hindbrain early in development made this an attractive system in which hypothesis could be tested.

The following discussion will be enhanced by a brief comment on nomenclature. Names in italics (*Hoxa1*) refer to the genes or the mRNA for the gene, while names in normal font (Hoxa1) refer to the protein product of the mRNA. *Hoxa1* is the first of the *Hox* genes to be expressed in the hindbrain (Murphy and Hill, 1991) and its expression appears to be directly regulated by a retinoic acid response element (RARE) (Frasch et al., 1995; Langston and Gudas, 1992). *Hoxb1* expression also appears to depend on

RAREs, an element on the 3' end of the gene (the end of the DNA without a phosphate) the which helps establish early expression (Marshall et al., 1994),  and a repressor element on the 5' end of the gene (the end of the DNA with a phosphate) which acts in r3 and r5 (Studer et al., 1994) and which appears to start altering gene expression around 8.0 days post coitus (dpc) in the mouse (R. Krumlauf, personal communication).  The early expression of *Hoxb1* is also dependent on Hoxa1 (Studer et al., 1998) with the cofactor pbx (Green et al., 1998; Phelan et al., 1995), but continued expression in r4 is controlled by a strong auto regulatory loop with the cofactors exd/pbx (Popperl et al., 1995) and prep1 (Berthelsen et al., 1998a).  *Hoxa1* is expressed to a rostral limit in the developing neural tube to the presumptive r3/r4 boundary at 7.75-8.0 dpc, but the expression then regresses, vanishing from the hindbrain by 8.5 dpc.  The expression of *Hoxb1* is very similar, except for the continued autoregulatory maintenance in r4 (Maconochie et al., 1996).  Hoxb1, pbx, and prep1 all have a hand in up-regulating *Hoxb2* in r4 (Ferretti et al., 2000; Maconochie et al., 1997), while the later r5 expression of *Hoxb2* is regulated by Krox20 (Nonchev et al., 1996a; Nonchev et al., 1996b; Sham et al., 1993).  In r5 *Krox20* appears to be repressed by Hoxa1 and Hoxb1, and expression of *Krox20* occurs in r5 after they retreat from the hindbrain around 8 dpc.  By 8.5 dpc expression of *Krox20* and *Hoxb2* can be detected in r5 (Barrow et al., 2000; Wilkinson et al., 1989).  Thus, the mouse *cis*-regulatory network can be drawn as in Figure 3.5 below.

The synthesis of this data into Figure 3.5 is a new result and has been received favorably by one of the leaders in the field (R. Krumlauf, personal communication).  The organization of the figure itself draws upon ideas presented in the literature, but several features of the diagram are novel and go beyond current representations.  For instance,

the activation and repression binding sites are correctly drawn in their relative positions
on the chromosome, with the exception of *Krox20* (as it is still unclear how the Hoxa1
and Hoxb1 repression mechanism works and where the components are). The horizontal
orientation of *Hoxb1* and *Hoxb2* highlights the fact that they appear on the same
chromosome, while the vertical orientation of *Hoxa1* and *Hoxb1* highlights the fact that
they are paralogs. *Krox20* is offset both vertically and horizontally, from all the other
genes, thus showing that it is not connected. This presentation brings a new depth to the
standard representations (*cf.* Davidson, 2001).

The figure also shows the complexity of the situation. Even though this system
was chosen because there was a readily identifiable network that had a minimum number
of inputs, the network is still very complicated and includes a nonlinear feedback term for
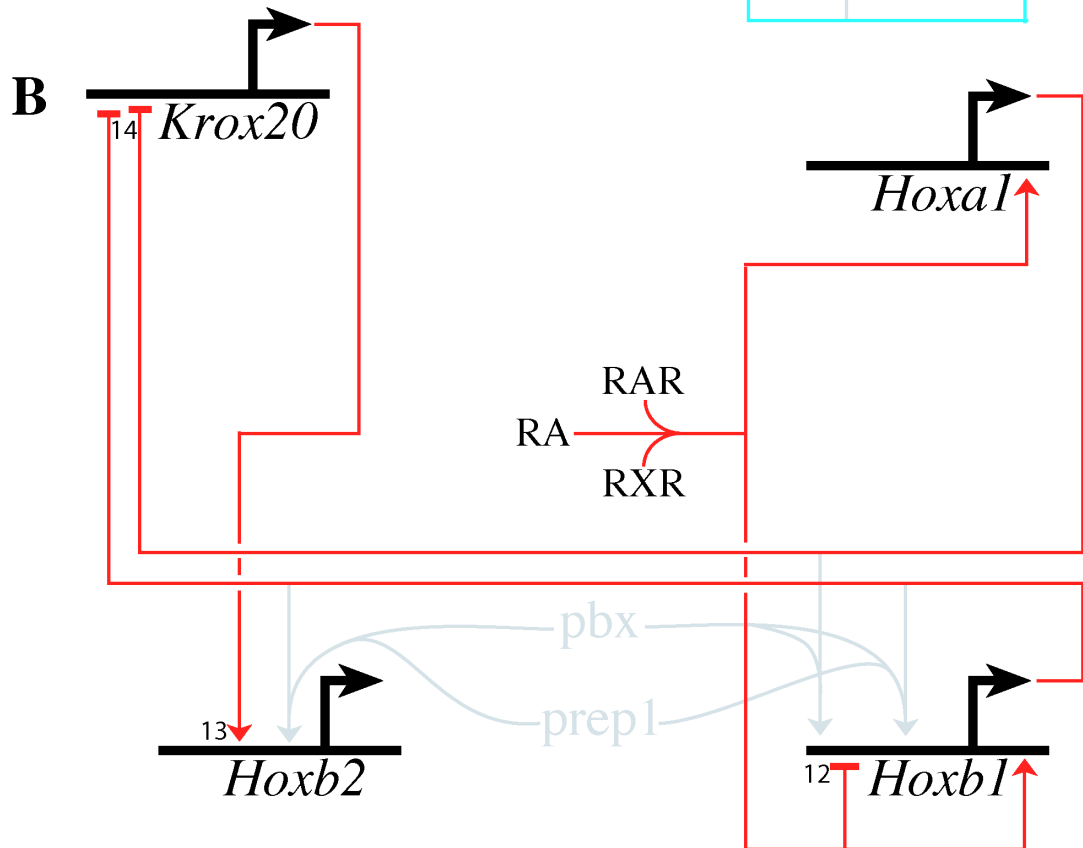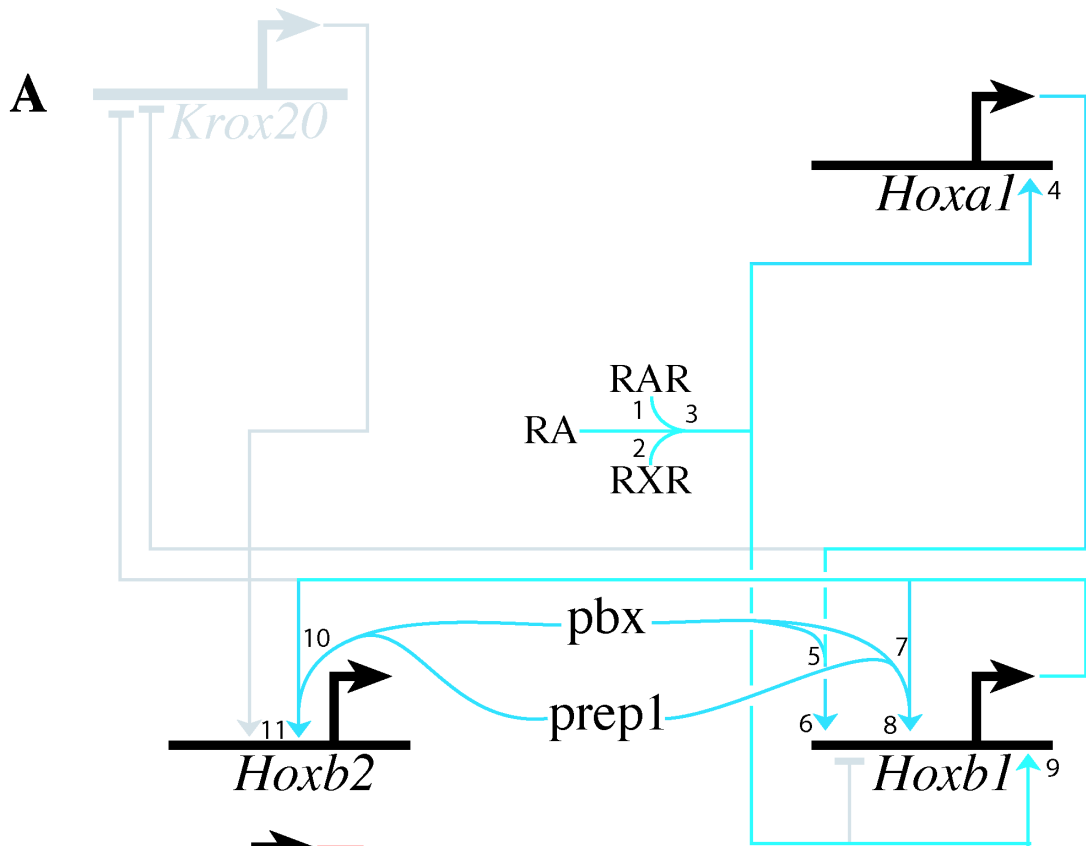the autoregulation of *Hoxb1*.

**Figure 3.5 *Hox cis*-regulatory network** in r4 **(A)** and r5 **(B)** The network is drawn in

a way to emphasize that (1) each cell contains the entire biochemical network, and (2)

certain interactions dominate in a particular rhombomere. Inactive elements are

denoted in gray. The numbers near each intersection refer to the references for the

interaction. **(A)** Starting with retinoic acid (RA) in the middle of the diagram, the RA

binds with RAR (1: (Petkovich et al., 1987) and RXR (2:(Leid et al., 1992a), which

can then form a dimer (3: (Leid et al., 1992b). The dimer can bind as a transcriptional

activator to *Hoxa1* (4: (Frasch et al., 1995; Langston and Gudas, 1992) or *Hoxb1* in r4

(9: (Marshall et al., 1994). The Hoxa1 protein, after binding with the pbx/prep1

complex (5: (Berthelsen et al., 1998b), can then bind as a transcriptional activator to

*Hoxb1* (6: (Studer et al., 1998). The Hoxb1 protein, in conjunction with pbx/prep1

can bind to *Hoxb1,* which provides an auto-regulatory mechanism (7,8: (Popperl et

al., 1995). The Hoxb1/pbx/prep1 complex can also bind as a transcriptional activator

to *Hoxb2* (10,11: (Maconochie et al., 1997). **(B)** The RAR/RXR dimer can bind as a

transcriptional activator to *Hoxa1* (4: (Frasch et al., 1995; Langston and Gudas, 1992)

or *Hoxb1* (9: (Marshall et al., 1994) in r5, and it can also bind as a transcriptional

repressor to *Hoxb1* (12: (Studer et al., 1994). Hoxa1 and Hoxb1 are hypothesized to

be transcriptional repressors of *Krox20* (14: (Barrow et al., 2000), while Krox20 is a

transcriptional activator of *Hoxb2* (13: (Sham et al., 1993).


While most of the *cis*-regulatory studies have been carried out in mice, chick has

proven to be a useful system for investigation of RA distribution. RA has long been

thought to be a diffusible morphogen that is able to pattern the hindbrain (Gavalas and

Krumlauf, 2000; Maden, 1999) and recent studies of RALDH-2 and CYP26, enzymes

important in RA synthesis and degradation, reveal expression patterns that continue to

support this view (Berggren et al., 1999; Swindell et al., 1999).  In addition, a RALDH-2

knockout shows effects similar to vitamin A deficiency (Niederreither et al., 1999).  More

direct tests of sensing this gradient in mouse or chick have been challenging; there has

been no conclusive evidence (Gavalas and Krumlauf, 2000).  Despite this lack of direct

evidence for a gradient, circumstantial evidence for it continues to accumulate.  Most

recently a study of RAR blocking by an antagonist has suggested that the establishment

of hindbrain boundaries is dependent on RA concentration (Dupe and Lumsden, 2001).

The work also suggested that the cells in the mid- and hindbrain are still responsive to

RA through stage10.  Therefore, RA cannot still be present in the midbrain and anterior

part of the hindbrain, otherwise genes that respond to RA—including *Hoxa1* and

*Hoxb1*—would be expressed in this region.  Thus, even if there is not an actual RA

gradient, there may be a graded response to retinoids, possibly involving other factors in

the system that help modulate the ability of the cell to respond to RA.  Taken together,

the evidence is suggestive that a differential of some sort, perhaps through RA

concentration, or through the temporally modulated ability to respond to RA, helps

establish the *Hox* gene patterns.

Because the SSA model is built on, and driven by, the underlying biochemistry of

the system, the reactions can be translated directly into the discrete events of the

simulations.  In this investigation, some of the steps of the system were deliberately

omitted.  For example, instead of creating explicit reactions for the transcription of

nuclear RNA, the splicing into mRNA, and the exporting of the mRNA to the cytoplasm, the simulation instead creates mRNA as a primary transcript. This is not unreasonable as long as the rate parameters $c_\mu$ are adjusted to reflect the subsequent delay, and as more data that describes these reactions is collected, these pieces can be easily incorporated at a later date.

Using Figure 3.5 as the network of interest, an SSA that described the *Hox* network system has been created using the C programming language. The source code for the model can be found in Appendix C and on the accompanying CD-ROM. The model contains 59 chemical events that can occur in each cell. They can be classified into 5 main categories: binding (including activation, repression, dimerization, and *Hox*/pbx/prep1 complex formation), unbinding, transcription, translation, and decay (of mRNA, dimers, complexes, proteins, and receptors). The two remaining events that do not fall into these categories are diffusion and division.

Of the 59 chemical events, most of them are first-order reactions. First-order reactions are ones with a single reactant, and so the rate of the reaction is proportional to the number of molecules. Therefore, the probabilistic rate for the stochastic simulation is of the form $a_\mu = c_\mu s_1$, where $s_1$ can be the number of mRNA available to be turned into proteins, or the number of molecules (including RA, mRNA, proteins, complexes, and receptors) available for decay. This is, of course, a simplified view of the true state of affairs in the cell. For instance, the mRNA cannot be translated into protein without the presence of a ribosome and the necessary amino acids, but these are assumed to be available in excess.

Zeroth-order reactions are ones that reactions that occur "spontaneously" and are not linked to any of the expressed genes in the simulation. Instead, they are considered as a stochastic event that can occur with some constant (low) probability and are governed by equations of the form $a_\mu = c_\mu$. One example of a zeroth-order reaction is the cell division function. The typical simulation encompasses 18 hours of developmental time and so the model includes a rudimentary mechanism for cell division and this is why the presumptive boundary sometimes shifts in the movies. When the division occurs, the resources in the cell are divided subject to a normal distribution between the daughter cells. The other zeroth-order reactions describe the creation of the RAR and RXR receptors and the pbx protein complex.

Second-order reactions involve two species of the simulation that combine and are of the form $a_\mu = c_\mu fg$, where $f$ is the number of molecules of the first species, and $g$ is the number of molecules of the second species. The four second-order reactions in the simulation describe RA binding to RAR, the binding of RA to RXR, the dimerization of the bound RAR and RXR forms, and the formation of the Hox/pbx/prep complexes. Because the species in these second-order reactions are different, there is no need to introduce a combinatorial factor as in Table 2.1.

There are a variety of ways to implement activation functions. These include binary activation, sequential activation, proportional activation, and Hill functions. A binary activation would be when a single transcription factor binds to the gene, thus creating an "activated" form of the gene. This activated form is then primed for the transcription of mRNA. Because of the large binding coefficients that accompany

transcription factors and DNA, even a small number of molecules of a transcription factor are enough to enable transcription. However, they must be present in sufficient numbers to establish a steady state in the binding/dissociation reactions.

Yet another way of implementing a transcription function is to assume that the probability of transcription is proportional to the number of transcription factor molecules. In other words, $a_\mu = c_\mu fg$ but in this case $g$ is either 1 if a gene is available for transcription or 0 if the gene is not available for transcription, and $f$ is the number of transcription factor molecules present. This form doesn't assume an explicit notion of an activated gene.

In the first incarnation of the model, the activation and repression functions are implemented using a Hill function (Hill, 1910), a typical way to represent cooperative binding. This takes the general form $a_\mu = c_\mu \frac{f^h}{\kappa_\mu + f^h} f \cdot g$, where $f$ is the number of molecules of a particular transcription factor, $\kappa_\mu$ is a threshold factor, and $g$ is the number of molecules of a gene available. Similar to the proportional case, if a gene is currently unbound, the value of $g$ is 1, while if it is bound by a transcriptional factor the value of $g$ is 0. The exponent $h$ is called the Hill coefficient and it affects the steepness of the response. The Hill function is an empirically derived expression, used in differential equation models, that yields the observed kinetics in these situations. Thus, in the stochastic reaction approach the complete Hill function expression is treated as simply another rate coefficient for the purposes of converting it to the appropriate probability of occurrence of the corresponding reaction. Others have used a similar method in their stochastic description of gene transcription (Arkin et al., 1998).

When it comes to the activation of *Hoxb1* in r4, there are actually two transcription factors that can bind to the gene. This is implemented using a variety of gene states controlled by a combination of Hill functions and sequential activations. *Hoxb1* is initially up-regulated by the RA dimers and the cross activation by *Hoxa1*. Therefore if one of those two factors is bound, the gene is marked as in an activated state, but if both are bound, the gene is marked as "superactivated." Each of those two activated states carries its own probability of transcription, with the superactivated form much higher. Maintenance is controlled by the *Hoxb1* auto-regulatory loop, and once the *Hoxb1* protein is present in sufficient numbers, auto activation can occur, again with an associated probability of transcription.

Diffusion is yet another first order reaction, and more molecules of RA means that there is greater chance of a diffusion event occurring. But the diffusion is secondary to the actual creation of the RA, and that needs to be treated with some care.

## Retinoic Acid Source

In the course of considering different ways that RA might pattern the hindbrain, a paper appeared that provided additional insight (Dupe and Lumsden, 2001). This work suggested that cells in the hindbrain are less able to respond to RA over time. This is not inconsistent with the previously mentioned investigations that suggest a physical variation in RA patterns the hindbrain (Gavalas and Krumlauf, 2000; Maden, 1999), but it does make modeling the system more challenging. Taken together, these studies propose that a variation of some sort (either temporal or spatial or possibly both) is an

important component in patterning the hindbrain, and provided support of some of the hypotheses used to construct the model.

There are two main ways that this variation can be implemented. The first is to create cells that are less responsive to RA over time, and the second is to create a variation in the RA. The model was built to allow for both of these possibilities. There is more evidence for a physical variation however, and the modeling efforts reflect this fact.
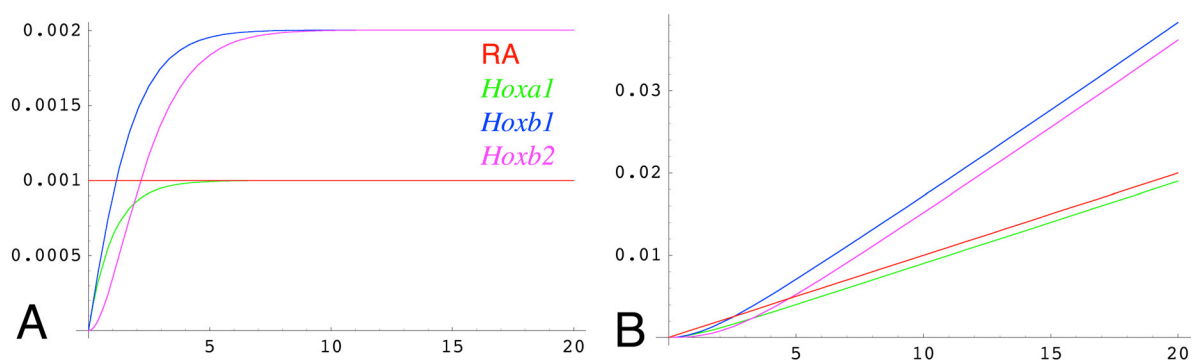
There are a variety of possible functions that can be used for modeling a physical variation of RA and many forms were considered. In Equations 3.1 are a set of differential equations derived from the Law of Mass Action that captures part of the network. While this formulation is problematic in general, especially for situations such as these with the low levels of the transcription factors, it was useful in quantifying the effects on the *Hoxa1*, *Hoxb1* and *Hoxb2* due to different RA source terms. Briefly, the rate of change of *Hoxa1* $(A_1)$ is dependent upon the creation effects of RA, and the depletion effects $(-\phi A_1)$ caused by normal decay or use as an up-regulator for *Hoxb1* $(B_1)$. Positive effects for *Hoxb1* include RA, the up-regulation by *Hoxa1* $(\alpha A_1)$ and the Hill auto-regulatory loop, while the depletion effects $(-\beta B_1)$ are caused by normal decay or its use as an up-regulation for *Hoxb2* $(B_2)$. The rate of change of *Hoxb2* is up-regulated by the amount of *Hoxb1* $(\delta B_1)$, and depleted by decay processes $(-\varepsilon B_2)$.

$$\frac{dA_1(t)}{dt} = RA(t) - \phi A_1(t)$$

$$\frac{dB_1(t)}{dt} = RA(t) + \alpha A_1(t) - \beta B_1(t) + \gamma \frac{B_1^2(t)}{1 + B_1^2(t)} \qquad (3.1)$$

$$\frac{dB_2(t)}{dt} = \delta B_1(t) - \varepsilon B_2(t)$$

**Equations 3.1 A simplified set of equations describing the behavior of the rhombomere 4 gene network.** Note that in this description there is only one cell, and this cell contains only 4 products and 6 reactions. This is a dramatic simplification from the full simulation of the 40 cells, each containing 30 products and 59 chemical reactions. But because the full simulation contains these basic reactions as well, this reduced set provided insight into the possible effects of different RA source terms.

A variety of different functions were considered for the RA source, and Figure 3.6 shows the trajectories of the solutions. The x-axis is time, and the y-axis is concentration. It is important to keep in mind that the experimental results in rhombomere 4 show that the *Hoxa1* mRNA increases then decreases, while the *Hoxb1* and *Hoxb2* mRNA reach a steady state. Therefore, the solutions that exhibit this behavior are the most interesting.

**Figure 3.6 A-H Response curves for various RA functions**. A variety of functions were investigated for the RA source term using the simplified network described in Equation 3.1. The legends for the plots **(B-H)** are the same as in **(A)**: RA in red, *Hoxa1* in green, *Hoxb1* in blue, and *Hoxb2* in magenta. The response curves were qualitatively the same for a wide range of the parameters. The parameters used to generate these particular plots were $\varphi = \alpha = \beta = \delta = 1, \gamma = 2, \varepsilon = 1/2$. **(A)** The source

term $RA(t) = .001$ causes the cell to create a constant amount of RA over time. This causes the *Hoxa1* to increase to the same level as the RA source and is therefore not an appropriate model for the RA source. **(B)** A linearly increasing RA source term ($RA(t) = .001t$) results in all the *Hox* genes to increase linearly over time, while **(C)** a linearly decreasing source term ($RA(t) = 1 - .05t$) results in the *Hox* genes to decrease over time after an initial surge in *Hoxb1* and *Hoxb2* because of the auto-regulatory loop. Both of these are expected, and neither is appropriate. **(D)** The investigation took an interesting turn when the RA was modeled with the step function $RA(t) = \text{UnitStep}[2 - t]$. This resulted in the right type of qualitative behavior, namely, a surge or *Hoxa1* and steady state levels of *Hoxb1* and *Hoxb2*. Two of the problems with this include the square non-biological source term and the sharp response from the *Hoxa1*. But two other functions **(E)** $RA(t) = e^{-t}$, a decaying exponential, and **(F)** a quadratic decay $RA(t) = \dfrac{1}{1 + t^2}$, produced very nice qualitative results. The *Hoxa1* increased then decreased, and the *Hoxb1* and *Hoxb2* reached a steady state due to the *Hoxb1* auto-regulatory loop. In addition, both of these have a RA source that diminishes smoothly over time. The only problem with using a source term from one of these families is that they both start at $t = 0$ with a large amount of RA immediately. This is not possible biologically, but the following two functions do exhibit behavior that can occur biologically as they both exhibit a smooth ramp-up as well as a smoothly diminishing tail. **(G)** A Gaussian curve of the general form $RA(t) = e^{-(t-\pi)^2/2}$ or a Rayleigh function like **(H)** $RA(t) = te^{-t}$ meet all the desired criteria. Ultimately, the Rayleigh function was chosen because of the

connection to other biological sources like insulin, which has a biphasic response

with a strong initial response and a longer continuing source (Rorsman et al., 2000).

A Rayleigh function was ultimately chosen to model the diffusion source term for

RA from the posterior of the embryo. This is implemented by having the first cell create

the RA according to the probabilistic rate $a_0 = c_0 \cdot RA_0 \tau e^{-\alpha \tau^2}$ where $RA_o$ is the initial

amount of RA in the system, and $\alpha$ controls the decay time of the source.

## Parameters

Using appropriate values for the model parameters is an important component in

modeling the system behavior. Fortunately, several key parameters are known, but many

of the important parameters for the model have not been assayed directly in experiments

on the developing hindbrain. Estimates of many of their values can be made from data

obtained in other systems, and were used in selecting parameters here (Table 3.1).

| Event | $K_d$ | Reference |
| --- | --- | --- |
| RA binding to RAR | 0.5 nM | (Allegretto et al., 1993) |
| RA binding to RXR | 2 nM | (Allegretto et al., 1993) |
| RAR/RXR dimerization | 17 nM | (Depoix et al., 2001) |
| Dimer binding to *Hoxa1* | 3.8 nM | (Mader et al., 1993) |
| Dimer binding to *Hoxb1* | 5.3 nM | (Mader et al., 1993) |
| Hox/pbx/prep binding to DNA | 2 nM | (Pellerin et al., 1994) |

**Table 3.1** Various measured binding coefficients for the interactions of the components of the model. The measured values are not measured in the systems under investigation, namely mouse and chick, but in cell culture systems. For example, the $K_d$ value for RAR/RXR dimerization has been determined in HeLa cells. Because the $K_d$ value is the rate (in M) at which these complexes come apart, this is a first order reaction and so the stochastic "probabilistic rate" parameter $c_d$ is equal to $K_d$ (Gillespie, 1977). Note that these values are the ratio of the backwards to forward binding rate constants $c_b$ and $c_f$. This is a typical state of affairs: the values $c_b$ and $c_f$ are very difficult to measure. This allows a bit of leeway in picking the forward and backwards binding, but the literature provides some typical forward values which adds credence to the values used and listed in Table 3.2 (Lauffenburger and Linderman, 1993).

It is not expected that the model results will be significantly different when newly measured parameters are incorporated in place of the estimated values. A sensitivity analysis, in which the model is re-run with systematically varied parameters, shows that the model remain qualitatively unchanged for moderate changes in the parameters. This is encouraging, as biological systems are generally robust, and it would be unusual that the overall biological system would be overly sensitive to moderate changes in the concentrations or rates.

The half-lives for mRNA can range from minutes to hours and values for the *Hox* mRNA have not been measured. In this model the values of around 15-20 minutes were chosen as a typical half-life, numbers that are in line with other values in early

embryogenesis (Davidson, 1986). The half-lives of the proteins in the network have not

been measured and the values chosen were between 15 and 30 minutes. These numbers

are again in an acceptable range for transcription factors (A. Varshavsky, personal

communication). Similar values were used for the turnover of the receptors and

complexes. With respect to the number of RARs and RXRs, values of around one

thousand of each type were chosen (Lauffenburger and Linderman, 1993). No

distinction is made between the $\alpha$, $\beta$, and $\gamma$ forms. The cofactors pbx and prep1 are

treated as a single molecule, which the *Hox* proteins can bind with on the DNA.

| Parameter | Value used | Description | Equation Type |
|---|---|---|---|
| $c_0$ | 4.0 | Create RA | Rayleigh |
| $c_1$ | 10000000.0 | Bind RA to RAR | Second-order |
| $c_2$ | 0.00006 | Decay RA | First-order |
| $c_3$ | 0.0001 | Create RAR | Zeroth-order |
| $c_4$ | 0.00006 | Decay RAR | First-order |
| $c_5$ | 0.005 | Unbind RA from RAR | First-order |
| $c_6$ | 0.0004 | Decay BRAR | First-order |
| $c_7$ | 1000000000 | Bind dimer to *Hoxa1* DNA | Hill |
| $c_8$ | 3.0 | Unbind dimer from *Hoxa1* DNA | First-order |
| $c_9$ | 0.02 | Transcribe *Hoxa1* mRNA | First-order |
| $c_{10}$ | 0.0007 | Decay *Hoxa1* mRNA | First-order |
| $c_{11}$ | 0.005 | Translate *Hoxa1* protein | First-order |
| $c_{12}$ | 0.001 | Decay *Hoxa1* protein | First-order |
| $c_{13}$ | 100000000.0 | Bind dimer to *Hoxb1* DNA | Hill |
| $c_{14}$ | 0.5 | Unbind dimer from *Hoxb1* DNA | First-order |
| $c_{15}$ | 0.02 | Transcribe *Hoxb1* | First-order |
| $c_{16}$ | 0.001 | Decay *Hoxb1* mRNA | First-order |
| $c_{17}$ | 0.02 | Translate *Hoxb1* protein | First-order |
| $c_{18}$ | 100000000.0 | Bind *Hoxa1* complex to Hoxb1 DNA | Hill |
| $c_{19}$ | 0.3 | Unbind *Hoxa1* complex from *Hoxb1* DNA | First-order |
| $c_{20}$ | .02 | Transcribe *Hoxb1* protein | First-order |
| $c_{21}$ | 1000000.0 | Bind dimer to *Hoxb1* repression site | Hill |
| $c_{22}$ | 0.00003 | Unbind dimer from *Hoxb1* repression site | First-order |
| $c_{23}$ | 1000000000 | Bind *Hoxb1* complex to *Hoxb1* DNA | Hill |
| $c_{24}$ | 0.3 | Unbind *Hoxb1* complex from *Hoxb1* DNA | First-order |

| $c_{25}$ | 0.02 | Transcribe *Hoxb1* protein | First-order |
|---|---|---|---|
| $c_{26}$ | 0.004 | Decay *Hoxb1* protein | First-order |
| $c_{27}$ | 1000000.0 | Bind *Hoxb1* complex to *Hoxb2* DNA | Hill |
| $c_{28}$ | 0.03 | Unbind *Hoxb1* complex from *Hoxb2* DNA | First-order |
| $c_{29}$ | 0.02 | Transcribe *Hoxb2* mRNA | First-order |
| $c_{30}$ | 0.00001 | Decay *Hoxb2* mRNA | First-order |
| $c_{31}$ | 0.002 | Transcribe *Hoxb2* mRNA | First-order |
| $c_{32}$ | 0.004 | Decay *Hoxb2* protein | First-order |
| $c_{33}$ | 0.00000015 | Cell division | Zeroth-order |
| $c_{34}$ | 100000.0 | Activate *Krox20* | First-order |
| $c_{35}$ | 0.002 | Unactivate *Krox20* | First-order |
| $c_{36}$ | 0.2 | Transcribe *Krox20* mRNA | First-order |
| $c_{37}$ | 0.0003 | Decay *Hoxa1* mRNA | First-order |
| $c_{38}$ | 12000.0 | Bind *Hox* complex to *Krox20* repression site | Hill |
| $c_{39}$ | 0.003 | Unbind complex from Krox20 repression site | First-order |
| $c_{40}$ | 0.0001 | Translate *Krox20* protein | First-order |
| $c_{41}$ | 0.00001 | Decay *Krox20* protein | First-order |
| $c_{42}$ | 10000000.0 | Bind RA to RXR | First-order |
| $c_{43}$ | 0.0001 | Create RXR | Zeroth-order |
| $c_{44}$ | 0.00006 | Decay RXR | First-order |
| $c_{45}$ | 0.02 | Unbind RA from RXR | First-order |
| $c_{46}$ | 0.002 | Decay bound RXR | First-order |
| $c_{47}$ | 5000.0 | Bind BRXR to BRAR | Second-order |
| $c_{48}$ | 0.0001 | Unbind BRXR from BRAR | First-order |
| $c_{49}$ | 10.0 | Decay BRAR/BRXR dimer | First-order |
| $c_{50}$ | 10000000.0 | Bind *Hoxa1* protein to PBX complex | Second-order |
| $c_{51}$ | 0.02 | Unbind *Hoxa1*/PBX protein complex | First-order |
| $c_{52}$ | 0.009 | Decay *Hoxa1*/PBX protein complex | First-order |
| $c_{53}$ | 10000000.0 | Bind *Hoxb1* protein to PBX complex | Second-order |
| $c_{54}$ | 0.02 | Unbind *Hoxb1*/PBX protein complex | First-order |
| $c_{55}$ | 0.01 | Decay *Hoxb1*/PBX protein complex | First-order |
| $c_{56}$ | 0.01 | Create bare PBX complex | Zeroth-order |
| $c_{57}$ | 0.005 | Decay bare PBX complex | First-order |
| $K_1$ | 1000 | Threshold for ActivateA1 Hill function | N/A |
| $K_2$ | 1000 | Threshold for ActivateB1 Hill function | N/A |
| $K_3$ | 1000 | Threshold for SuperActivateB1 Hill function | N/A |
| $K_4$ | 10000 | Threshold for AutoActivateB1 Hill function | N/A |
| $K_5$ | 1000 | Threshold for ActivateB2 Hill function | N/A |
| $K_6$ | 100 | Threshold for repression functions | N/A |
| a1hill | 4.0 | Hill coefficient for ActivateA1 Hill function | N/A |
| b1hill | 4.0 | Hill coefficient for ActivateB1 Hill function | N/A |
| b1auto | 6.0 | Hill coefficient for AutoActivateB1 Hill function | N/A |
| b2hill | 2.0 | Hill coefficient for ActivateB2 Hill function | N/A |

| rephill | 4.0 | Hill coefficient for repression functions | N/A |
|---------|-----|-------------------------------------------|-----|

**Table 3.2 Parameters used in the simulation**. The type of reaction and the associated value used is listed. As examples, the function for binding RA to the retinoic acid Receptor RAR is $a_1 = 1 \times 10^7 \{RA\}\{RAR\}$ where $\{\ \}$ denotes the number of molecules of each type. The first order reaction of the *Hoxa1* mRNA decaying is given by $a_{10} = 7 \times 10^{-4} \{mHoxa1\}$, and the Hill activation of *Hoxb2* is given by

$$a_{27} = 1 \times 10^6 \frac{\{Hoxb1\,pbx\,complex\}^2}{\left(1 \times 10^6 + \{Hoxb1\,pbx\,complex\}^2\right)} * \{Hoxb1\,pbx\,complex\} * \{Hoxb2\,DNA\}$$

In implementing the repression of *Hoxb1*, the simulation started this mechanism around 8.0 dpc because of the current understanding that the repression starts later than the activation (R. Krumlauf, personal communication). The *Hoxa1* and *Hoxb1* repression for *Krox20* is also started at around 8.0 dpc to ensure the establishment of *Hoxa1* and *Hoxb1* before the *Krox20* expression.

## *Results*

The early *Hox* genes first appear around 7.75 dpc (headfold) and the patterns of *Hoxa1*, *Hoxb1, Hoxb2* and *Krox20* stabilize by 8.5 dpc (~10 somites). Using the network shown in Figure 3.5, the goal was to capture this wild-type expression. Accordingly, the model was run for a simulated time of 18 hours. The model is one dimensional along the rostral-caudal axis of the embryo. Running the simulation with different random number seeds show that the model is not overly sensitive to the initial seed values. In the figures,

a number of these independent runs are assembled side-by-side to construct a two-dimensional sheet of cells that resemble the tissue (with a medio-lateral dimension). This offers insights into the expected two-dimensional pattern of gene expression in the hindbrain and displays the variability in the results.

A custom built notebook in *Mathematica* (found in Appendix D) was used to display the results of the simulations. The raw data (the number of molecules of each type in each cell) has been scaled to numbers between 0 and 1 by dividing by the maximum value in that data set. This allows the creation of a color shading so that differences in levels of molecules are clear. The results are displayed in an easy to understand format: a virtual dynamic *in situ*. Because the maximum value used to scale the data is on the order of tens to a couple hundred molecules, the color variations that are seen in the figures and the movie may in fact be too small to distinguish in a laboratory setting using conventional *in situ* staining.

## Wild Type

Figure 3.7 presents the dynamics of the model concerning the emergence of *Hoxa1*, *Hoxb1*, *Hoxb2* and *Krox20*, over time from approximately 7.75 dpc to 8.5 dpc. The figure presents single frames from the movie wt.mov. Along with all the other movies referenced in this thesis, wt.mov can be found on the included CD-ROM. The movie offers a dynamic view of the mRNA and RA in the developing hindbrain. Each rhombomere starts out with 20 cells, and the presumptive boundary is clearly marked. Even though the movies and figures show the mRNA levels, the model also tracks the

amount of protein, bound and unbound complexes, and bound and unbound receptors,

and any of these data can be displayed in a similar manner.

The low levels of *Hoxa1*, *Hoxb1* and *Hoxb2* mRNA in r4 and r5 are first seen

soon after the simulation starts when the RA sweeps across the cells (Figure 3.7A).  After

the mRNA is translated into protein and subsequently forms a complex with pbx and

prep1, it can then bind to the DNA.  The effects of the *Hoxa1* binding site on *Hoxb1* and

the *Hoxb1* auto-regulatory loop are seen next, namely the higher levels of *Hoxb1* in r4

(Figure 3.7B).  By 8 dpc the RA has long since vanished from the hindbrain and

consequently the RAR/RXR dimers are no longer being created.  This is the main reason

that *Hoxa1* starts to vanish from the hindbrain.  The lack of available dimers also

contributes to *Hoxb1* vanishing from r5, as does the late repression mechanism (Figure

3.7C).  Now that *Hoxa1* and *Hoxb1* no longer repress *Krox20* in r5, its expression rises

and subsequently brings up *Hoxb2* in r5.  At about this time, *Hoxb2* has appeared in r4

due to the up-regulation by *Hoxb1* (Figure 3.7D).  The ending expression pattern of the

five genes at 8.5 dpc (Figure 3.7E) is very similar to reported patterns (Lumsden and

Krumlauf, 1996).

It is clear from laboratory data that cells sometimes "misfire," and using this

simulation it is possible to see the consequences of such misfirings.  In Figure 3.7, (A, B,

D, E) the cell marked with an arrow deviates from its normal fate and ends up not

expressing any genes.  At the same time, there are other cells that appear to misfire early,

exemplified by low levels of expression, but later recover.  This is exemplified by the

lone white cell in the r4 *Hoxb1* data at 8.15 dpc.  For whatever reason, it was not

expressing *Hoxb1* at this timepoint, but it recovers by 8.5 dpc.  Both of these events are

known to happen in biological systems, and it is encouraging to see this behavior in the

model, as these events are not captured with conventional modeling methods. This result

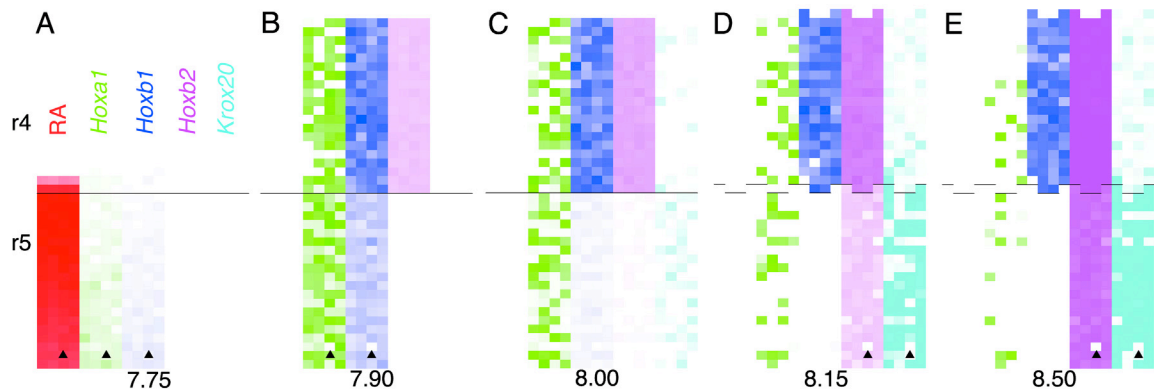suggests that fluctuations are a factor in the network under investigation.



**Figure 3.7 Simulated wildtype mRNA and RA patterns from 7.75 dpc to 8.5
dpc (A-E)** Selected frames from the computer generated time-lapse movie
wt.mov. Four runs of the simulation were required to create this picture, with each
run contributing a row of RA, *Hoxa1*, *Hoxb1*, *Hoxb2* and *Krox20* data for each
timepoint. Notice that sometime between 8 dpc and 8.15 dpc there is a cell
division in r5 in the first and fourth data sets. This can be seen most clearly in the
*Hoxb2* and *Krox20* data at 8.5 dpc. When a cell divides, its resources are
normally distributed between the daughter cells. The data for the marked cell was
generated during one of the simulations, and the consequences of this cell
misfiring can clearly be seen **(A)** At 7.75 dpc there is an abundance of RA and
low levels of both *Hoxa1* and *Hoxb1* expression are evident in the marked cell.
**(B)** The expression of *Hoxa1* and *Hoxb1* fades in this cell by 7.90 dpc, a bit
earlier than some of its neighbors. **(E)** By 8.5 dpc the cell has failed to initiate its

proper expression of *Krox20* and *Hoxb2*. This result suggests that fluctuations are important in the network under investigation.

## *In Silico* Experiments

The versatility of the computer simulation also allows for the possibility of performing *in silico* experiments. The results of two experiments are reported here and the simulation output shows that the results are similar to their corresponding *in vivo* experiments. In addition, the simulation suggests results that have not been reported in the laboratory, and these predictions warrant further investigation *in vivo*.

## *Hoxb1* Mutant

In the investigation of the cross-regulation of *Hoxb2* by *Hoxb1* in r4 (Maconochie et al., 1997), the authors showed that the up-regulation of *Hoxb2* in r4 is lost in *Hoxb1* mutants. Duplicating this experiment *in silico* requires a minimum number of changes to the model, and is accomplished by not allowing any transcription factors to bind to the *Hoxb1* DNA. The input parameters used were the same as in the wild type (Table 3.2). In stills taken from the movie Hoxb1mutant.mov, it starts as in the wild type: the RA comes through the hindbrain at 7.75 dpc and induces the expression of *Hoxa1*. However, because the *Hoxb1* gene is "turned off," there is no *Hoxb1* expression (Figure 3.8A). Later on, as reported in the literature, *Hoxb2* is absent from r4. It is also clear that *Krox20* fails to be well repressed in r4 (Figure 3.8B). By 8.5 dpc, *Hoxb1* expression is still absent and high levels of *Krox20* are firmly established in r4 (Figure 3.7C). This last result has yet to be thoroughly investigated, but there are two ways that this could be tested in the laboratory. The first is to acquire the mice used in the study and check the

*Krox20* expression, while the second is to create a DNA construct that mimics this type of behavior in chick. Acquiring the mutant mice is not an easy, quick, or inexpensive task, and so the second approach was taken. The attempt to perform this perturbation experiment is fully described in Appendix A.
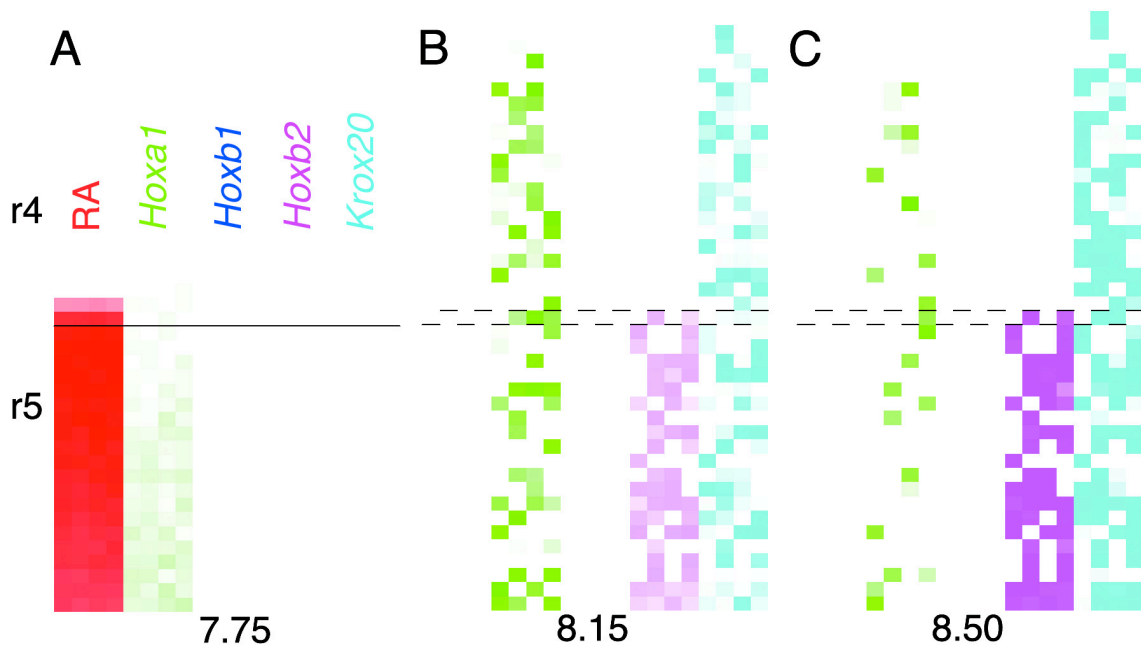


**Figure 3.8 Simulated *Hoxb1* mutant mRNA expression patterns. (A-C)**

Selected frames from the computer generated time-lapse movie Hoxb1mutant.mov. This data set shows cell division having occurred in both r4 and r5. Besides affecting the *Hoxb2* expression in r4, the *Hoxb1* mutant also has an effect on *Hoxb2* and *Krox20* in r5. **(B)** The levels of *Krox20* are lower at 8.15 dpc than in the wild-type (Figure 3.6D). **(C)** By 8.5 dpc, the levels of *Krox20* and

*Hoxb2* are noticeably lower than the wild type (Figure 3.6E). The observation on the level of *Krox20* expression is a prediction that can be tested in the laboratory.

## 5' RARE Mutant

The effects of a selected deletion in the *Hoxb1* 5' RARE showed that the RARE plays a role in the r4 restricted expression of *Hoxb1* (Studer et al., 1994). In this work the authors showed that if the construct lacked the 5' RARE, the reporter expression spread to r3 and r5. Further study suggests that the r3/r5 repressor region that contains the RARE is activated later than the 3' enhancer element (R. Krumlauf, personal communication). Duplicating this experiment using the model is again a simple matter, and is accomplished by not turning on the repressor. As in the *Hoxb1* mutant experiment described above, the parameters used were the same as in the wild type (Table 3.2). The stills from the movie RAREmutant.mov show that the expression pattern looks normal at 7.75 dpc (Figure 3.9A). However, at 8.0 dpc the repression mechanism is not turned off, and by 8.15 dpc the expression of *Hoxb1* in r5 is still strong (Figure 3.9B). By 8.5 dpc, the *Hoxb1* expression has faded in r4 somewhat due to the lack of available RAR/RXR dimers, but is still noticeable (Figure 3.9C). In addition, there is once again a change in the pattern of *Krox20*, but this time there are lower expression levels in r5 (Figure 3.9C). This is due to the continued repression effects of *Hoxa1* and *Hoxb1*. This result has yet to be fully investigated in the laboratory.
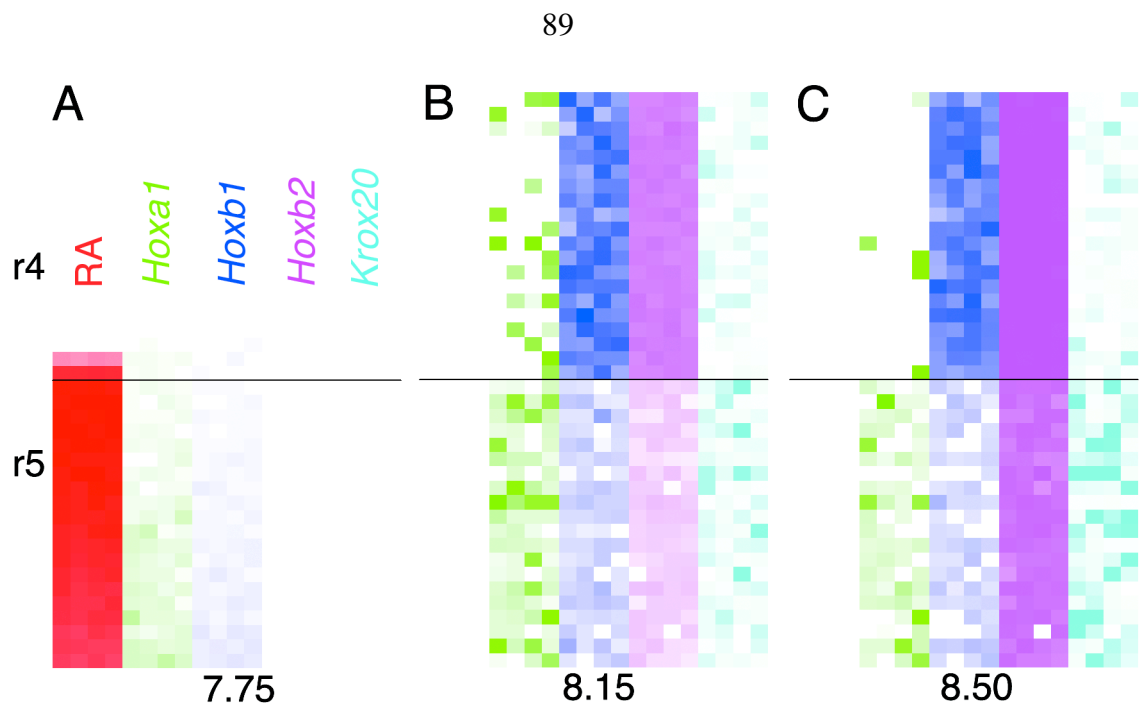
**Figure 3.9 Simulated expression patterns after inactivation of the 5' *Hoxb1***

**RARE (A-C)** Selected frames from the computer generated time-lapse movie

RAREmutant.mov.   By turning off the 5' RARE, there is a change in the levels

of *Hoxa1* expression in r5.  This occurs because the 3' and 5' RAREs are in effect

fighting for the RAR/RXR dimers.  This intriguing result needs to be more fully

investigated.  As in the wild type, it is easy to see downstream effects from cells

that have misfired, most notably the patches where *Hoxa1* or *Hoxb1* are

continuing to repress *Krox20*.  **(A)** The behavior of the system mimics the wild-

type at 7.75 dpc because the 5' RARE does not kick in until 8 dpc. **(B)** By 8.15

dpc, the expression of *Hoxb1* is still noticeable in r5, but the levels are low

enough to allow *Krox20* expression to take hold.  **(C)** The levels of *Krox20* in r5

are higher than in the wild type (Figure 3.7E). The effects of the *Hoxb1* RAREs

not having to compete for the dimers is clear by 8.5 dpc as evidenced by the

higher levels of *Hoxa1* as compared to the wild type (Figure 3.7E).

## *Sensitivity Analysis*

A model that is presented with no analysis leaves something to be desired, and

this section presents the results of a sensitivity analysis. There are two categories of

conventional analysis possible: local and global sensitivity analysis. Local analysis is

based upon evaluating the derivative of some output function with respect to any of the

input variables at some fixed point in the space of the input variables. However, this

approach is only really practical for linear models, and a local analysis is unable to gauge

the impact of possible differences in the scales of the variations of the input variables. It

has been recognized for several decades that when the model is nonlinear and the various

input values are affected by uncertainties of different orders of magnitude, a global

sensitivity analysis should be used (Cukier, 1973).

Recall that the simulation consists of over 75 input parameters, and the output

consists of the quantities of 19 different molecular species for each of forty cells cell at

each of the1080 time points, or over 800,000 outputs. Doing a sensitivity analysis over

all these parameters would prove intractable. Because of this, the data was compacted

before the analysis was run.

First of all, each of the 40 cells is assigned either an r4 or an r5 identity, and so

the cells were grouped by their rhombomeric identity and the number of molecules for

each species was averaged over all the cells. Next, since the movies and the experiments

are primarily concerned with the amount of messenger RNA that is in these cells, special attention was focused on the mRNA and how the variation in the parameters affected these quantities. Finally, instead of looking at 1080 time points, the data was downsampled to 54 time points (one for every 20 minutes instead of every minute).

## Measure of Importance

The global analysis initially tried is one that is based on a "measure of importance" called S. In this type of approach, all the parameters are varied simultaneously and the sensitivity of the output variables is measured over the entire range of each input parameter. It allows the output variance to be broken up into contributions due to individual parameters or combinations of parameters (Homma, 1996). As an illustrating example, let $\mathbf{y} = f(\mathbf{x})$ be the black box of the simulation to be evaluated, where $\mathbf{x} = (x_1, x_2, x_3)$, and $\mathbf{y}$ is an output vector of size m. Suppose the total variance of $f(\mathbf{x})$ is V. It is possible to write V as a sum of the variances that contribute to the total

$$V = V_1 + V_2 + V_3 + V_{12} + V_{23} + V_{13} + V_{123} \tag{3.2}$$

Then $S_1 = V_1 / V$ is the fraction of the total variance due to the parameter $x_1$ averaged over all the parameters and it is called the first order term for the parameter $x_1$. In a similar vein, $S_{12} = V_{12} / V$ is the fraction of the total variance due to the coupling of the parameters $x_1$ and $x_2$ and is called the second order term for the parameters $x_1$ and $x_2$. These variables can be combined to produce the sensitivity indices for each of the input variables by computing

$$S_{T,1} = S_1 + S_{12} + S_{13} + S_{123} \qquad\qquad (3.3)$$

Calculating these variables is a straightforward, albeit time-consuming exercise. Notice that the $S_i$ are all positive and sum to one, with the most important factors having the largest contribution.

This analysis was performed on the model and the results were not surprising. In Table 3.3 are several sensitivity indices computed for the mRNA in each of the rhombomeres.

| Parameter | Rhombomere | $S_i$ value for mRNA for | | | | |
| | | *Hoxa1* | *Hoxb1* | *Hoxb2* | *Krox20* | Sum |
| --- | --- | --- | --- | --- | --- | --- |
| $K_1$ | 4 | 0.25390 | 0.06763 | 0.04099 | 0.10119 | 4.18192 |
| | 5 | 0.04755 | -0.02082 | 0.01945 | 0.00594 | -0.04203 |
| $c_1$ | 4 | -0.33742 | -0.47741 | -0.47995 | -0.40615 | -5.43707 |
| | 5 | -0.37504 | -0.37020 | -0.49049 | -0.47657 | -6.16916 |
| $c_{13}$ | 4 | 0.34952 | 0.06243 | 0.04217 | 0.07847 | 4.78133 |
| | 5 | 0.36623 | -0.09437 | 0.02032 | 0.00078 | 1.03525 |
| $c_{26}$ | 4 | 0.11857 | 0.12154 | 0.06911 | 0.07454 | 3.90804 |
| | 5 | -0.03849 | 1.13157 | 0.02944 | 0.09681 | 1.58401 |

**Table 3.3 Sensitivity Analysis using the Measure of Importance**. This analysis does not appear to be one that can be employed for a simulation that is subject to stochastic variations.

In direct defiance of the theoretical analysis, the $S_i$ values are not all positive and they do not sum to one. The result of this analysis confirmed an important aspect of the model: the inherent fluctuations of the system can at times have stronger effects than a change in a parameter, and the stochasticity of the simulation plays a synergistic role with the change of the parameters. Accordingly, this type of analysis does not seem to address the question at hand, and it another type of analysis was used to examine the effects of changing the parameters.

## Excess Variance

Because the simulation is fundamentally subject to fluctuations, it is challenging to determine the effect on the output due to a change in a parameter. But this can be addressed using an excess variance based analysis. Let $v_j(\mathbf{x}, t)$ denote an output of interest from the simulation at time $t$ with input vector $\mathbf{x}$ and random number seed $j$. Let $v(\mathbf{x}; x_i, t)$, denote the output from the simulation at time t with the input value $x_i$ perturbed but all other inputs the same, and the default random number seed. Computing the mean of the squared difference of these values,

$$E_j\left[\left(v_j(\mathbf{x}, t) - v(\mathbf{x}; x_i, t)\right)^2\right] \tag{3.4}$$

yields a response curve. This value is a consistent estimator (*i.e.*, the probability of the estimated value and the true value of the population parameter not lying within any arbitrary positive constant c units of each other approaches zero as the sample size tends

to infinity), and identifies the parameters that have an important effect in contributing to the output values of interest.

This calculation was performed for the levels of mRNA for *Hoxa1*, *Hoxb1*, *Hoxb2* and *Krox20*. The analysis was only performed for the $c_\mu$ values because previous investigations while building the model had shown that these were the most important in determining the system behavior. The analysis was performed for each of the 4 target variables, for each of the rhombomeres, and to allow for legibility of the plots, the $c_\mu$ values were examined 10 at a time. This resulted in a total of 48 figures, but in the interest of space, not all of the plots are shown. Typical plots of these results are shown in Figures 3.10, 3.11 and 3.12 below, and the results of the entire investigation are summarized in Table 3.4.

Figure 3.10 shows the normal state of affairs; none of the $c_\mu$ ($\mu = 40\ldots49$) values plays a significant role in the expression of the messenger RNA for *Hoxb1* in rhombomere 4. But compare this plot to Figure 3.11. In this figure it is clear that $c_{53}$ plays a noticeable role on the level of mRNA for *Hoxb1* in rhombomere 4.
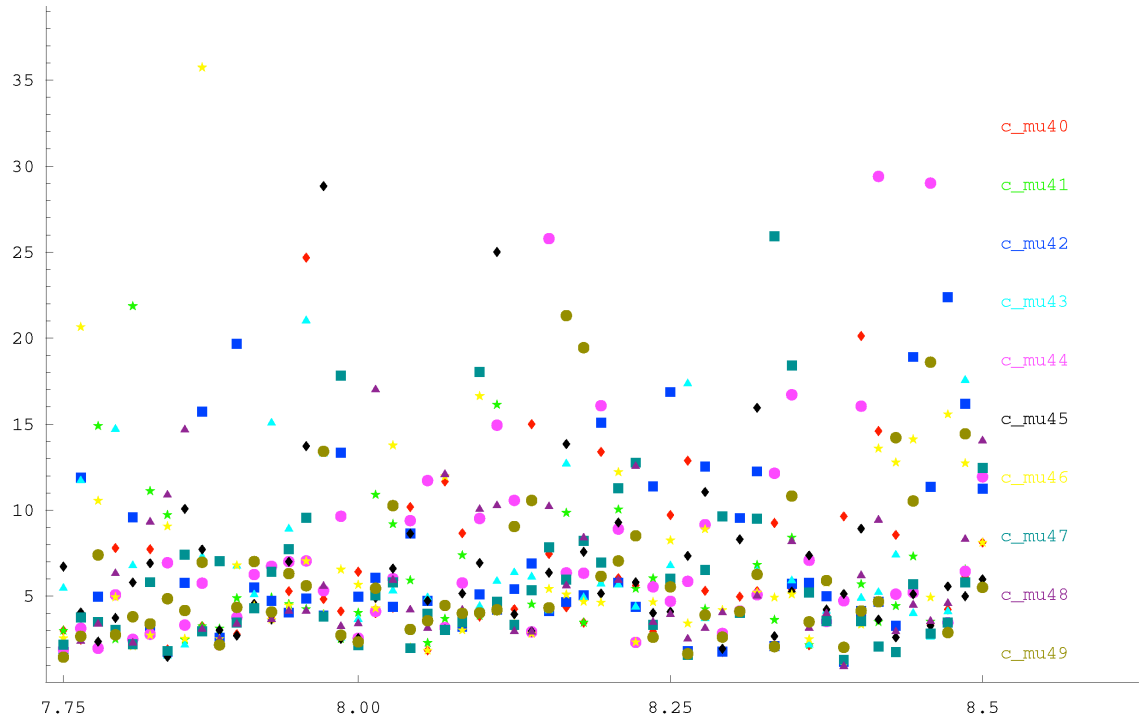
**Figure 3.10** Effects of $c_{\mu}$ values on mRNA for *Hoxb1* expression in rhombomere 4. The legend denotes the color of the response for a particular parameter, and in this instance none of the parameters has a significant effect. The x axis is time (dpc), and the y axis is the response value (computed in 3.4).
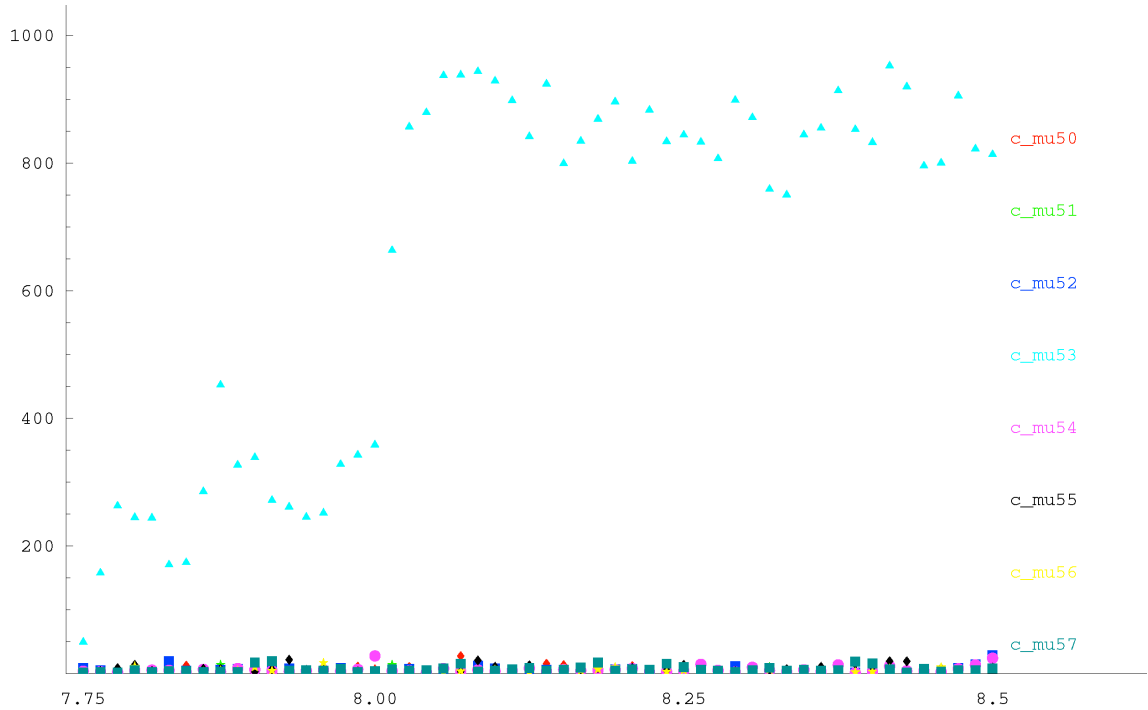
**Figure 3.11**: Effects of $c_\mu$ variables on the amount of mRNA for *Hoxb1* in rhombomere 4. The parameter $c_{53}$, which is part of the auto-regulatory loop, is by far the dominant parameter in this set. The x axis is time, and the y axis is the mean response values (computed in 3.4).

Looking at the list of values, $c_{53}$ is the stochastic rate coefficient for the formation of the *Hoxb1* protein/pbx/end complex, *i.e.*, $c_{53}$ is part of the auto-regulatory loop for *Hoxb1*, and it is no surprise that this parameter makes a difference in the expression of mRNA for *Hoxb1*. Compare this to Figure 3.12, which shows the effects of the same $c_\mu$ values on the mRNA for *Hoxb1*, but this time in rhombomere 5 in which there is no auto-

regulatory loop for *Hoxb1*. The contributions of the values are lower overall, and the

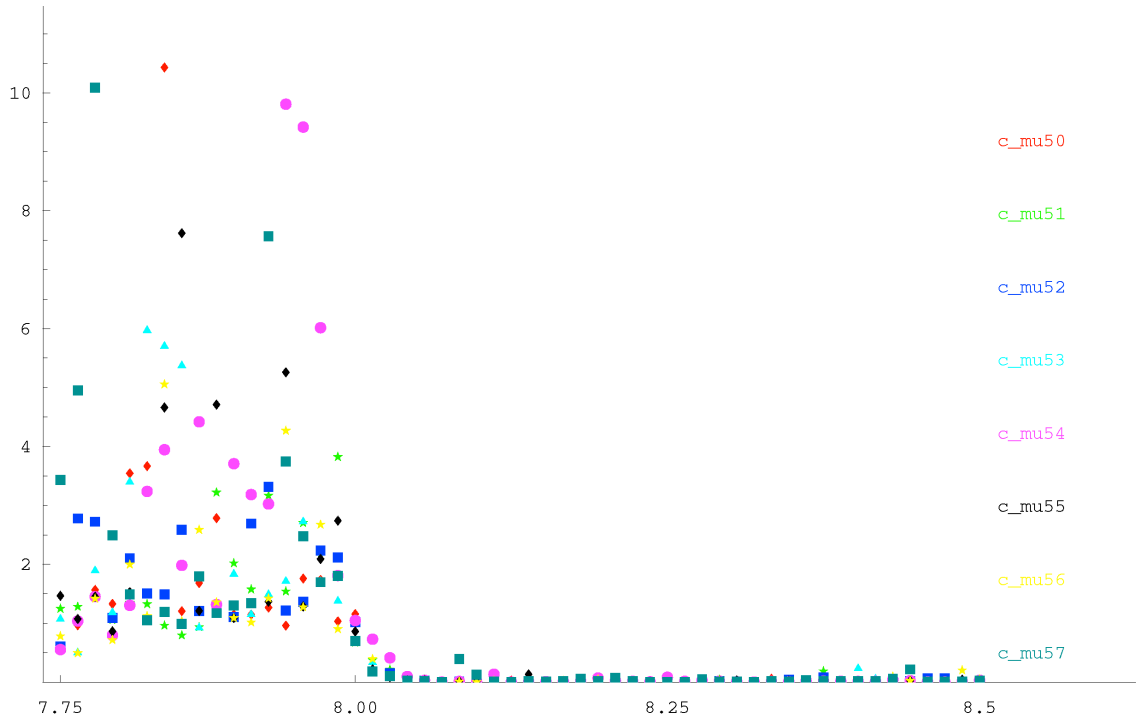repression mechanisms that turns on at day 8.0 makes a noticeable difference.



**Figure 3.12**: Effects of $c_\mu$ variables on the amount of mRNA for *Hoxb1* in

rhombomere 5. Notice that none of the parameters has a major effect on the

mRNA levels, and when the repression mechanisms start at 8 dpc, all of the

effects virtually vanish. The x axis is time, and the y axis is the mean response

values (computed in 3.4).

The $c_\mu$ values that play a role on the levels of the target variable are not

surprising. For instance, the transcription of mRNA for *Hoxa1* from the activated form

of the gene is important in both rhombomeres.

| Target | Rhombomere | Significant $c_\mu$ value | Related Function |
|--------|------------|---------------------------|------------------|
| *Hoxa1* | 4 | $c_7$ | ActivateA1 |
|         |   | $c_9$ | TranscribeA1 |
|         |   | $c_{10}$ | DecaymA1 |
|         | 5 | $c_7$ | ActivateA1 |
|         |   | $c_9$ | TranscribeA1 |
|         |   | $c_{49}$ | DecayDimer |
| *Hoxb1* | 4 | $c_{16}$ | DecaymB1 |
|         |   | $c_{25}$ | TranscribeAutoB1 |
|         |   | $c_{53}$ | Complexb1 |
|         | 5 | $c_{15}$ | TranscribeB1 |
|         |   | $c_{16}$ | DecaymB1 |
| *Hoxb2* | 4 | $c_{12}$ | Decaya1 |
|         |   | $c_{29}$ | TranscribeB2 |
|         |   | $c_{30}$ | DecaymB2 |
|         |   | $c_{53}$ | Complexb1 |
|         | 5 | $c_{16}$ | DecaymB1 |
|         |   | $c_{29}$ | TranscribeB2 |
|         |   | $c_{30}$ | DecaymB2 |
| *Krox20* | 4 | $c_{17}$ | Translate SuperB1 |
|          |   | $c_{53}$ | Complexb1 |
|          | 5 | $c_{25}$ | TranscribeAutoB1 |
|          |   | $c_{37}$ | DecaymKrox |

**Table 3.4**: **Effects of $c_\mu$ variables on the mRNA**. None of these variables is a great surprise. For instance, the parameters that change the mRNA for *Hoxb1* in r4 more than 20% above the baseline are the ones that affect the rate of decay of the mRNA for *Hoxb1*, the strength of the auto-regulatory loop, and the rate of Hoxb1/Prep complex formation. This last one might seem a little odd at first, until it is noted that the formed complex is required for the triggering of the auto-regulatory loop.

## *Summary*

The stochastic simulation model captures the timing of several *Hox* gene expression patterns in wild-type animals, and *in silico* simulations performed as a check of key interactions produced results similar to *in vivo* experiments. In addition, the *in silico* experiments yield intriguing results that bear further investigation in the laboratory.

The model simulations suggest that a transitory early release of RA may be sufficient to initiate the *Hox* genes. During the investigation of functions for modeling the RA source, it became clear that initiation of the network only required the RA source to stay on for as few as 3 minutes. All that was needed was enough RA to bind the receptors in r4 and r5 and proper expression of the target genes was the result. This refinement of the RA gradient hypothesis fits well with recent work on blocking RAR with a chemical antagonist in which the authors made a careful study of concentration and time dependent effects of the blocking agent using morphology and gene expression as assays. Chick embryos treated with the agent at HH stage 6 (Hamburger and Hamilton, 1951) do not express *Krox20* in r5, but treatment at HH stage 7 permits r5 expression (Dupe and Lumsden, 2001). Thus, the *Krox20* insensitivity to a later change in RA fits well with our model predictions: once the network was established early on proper r5 expression of *Krox20* was evident.

## *References for Chapter 3*

Allegretto, E. A., McClurg, M. R., Lazarchik, S. B., Clemm, D. L., Kerner, S. A., Elgort, M. G., Boehm, M. F., White, S. K., Pike, J. W., and Heyman, R. A. (1993). Transactivation properties of retinoic acid and retinoid X receptors in mammalian cells and yeast. Correlation with hormone binding and effects of metabolism. *J Biol Chem* **268,** 26625-33.

Arkin, A., Ross, J., and McAdams, H. H. (1998). Stochastic kinetic analysis of developmental pathway bifurcation in phage lambda-infected *Escherichia coli* cells. *Genetics* **149,** 1633-48.

Barrow, J. R., Stadler, H. S., and Capecchi, M. R. (2000). Roles of Hoxa1 and Hoxa2 in patterning the early hindbrain of the mouse. *Development* **127,** 933-44.

Bell, E., Wingate, R. J., and Lumsden, A. (1999). Homeotic transformation of rhombomere identity after localized Hoxb1 misexpression. *Science* **284,** 2168-71.

Berggren, K., McCaffery, P., Drager, U., and Forehand, C. J. (1999). Differential distribution of retinoic acid synthesis in the chicken embryo as determined by immunolocalization of the retinoic acid synthetic enzyme, RALDH-2. *Dev*. *Biol*. **210,** 288-304.

Berthelsen, J., Zappavigna, V., Ferretti, E., Mavilio, F., and Blasi, F. (1998a). The novel homeoprotein Prep1 modulates Pbx-Hox protein cooperativity. *Embo J* **17,** 1434-45.

Berthelsen, J., Zappavigna, V., Ferretti, E., Mavilio, F., and Blasi, F. (1998b). The novel homeoprotein Prep1 modulates Pbx-Hox protein cooperativity. *Embo. J.* **17,** 1434-45.

Cukier, R. I., Fortuin, C.M., Schuler, K.E., Petschek, A.G., and Schaibly, J.K. (1973). Study of the sensitivity of coupled reaction systems to uncertainties in rate coefficients, part I. *Journal of Chemical Physics* **59,** 3873-3878.

Davidson, E. H. (1986). "Gene activity in early development." Academic Press, Orlando.

Davidson, E. H. (2001). "Genomic Regulatory Systems." Academic Press, San Diego.

Depoix, C., Delmotte, M. H., Formstecher, P., and Lefebvre, P. (2001). Control of retinoic acid receptor heterodimerization by ligand-induced structural transitions. A novel mechanism of action for retinoid antagonists. *J. Biol. Chem.* **276,** 9452-9.

Duboule, D. (1994). Guidebook to the Homeobox Genes. Sambrook & Tooze, Oxford.

Dupe, V., and Lumsden, A. (2001). Hindbrain patterning involves graded responses to retinoic acid signalling. *Development* **128,** 2199-208.

Ferretti, E., Marshall, H., Popperl, H., Maconochie, M., Krumlauf, R., and Blasi, F. (2000). Segmental expression of Hoxb2 in r4 requires two separate sites that integrate cooperative interactions between Prep1, Pbx and Hox proteins. *Development* **127,** 155-66.

Frasch, M., Chen, X., and Lufkin, T. (1995). Evolutionary-conserved enhancers direct region-specific expression of the murine Hoxa-1 and Hoxa-2 loci in both mice and Drosophila. *Development* **121,** 957-74.

Fraser, S., Keynes, R., and Lumsden, A. (1990). Segmentation in the chick embryo hindbrain is defined by cell lineage restrictions. *Nature* **344,** 431-5.

Gallera, J. (1971). Primary induction in birds. *Adv*. *Morphogenet*. **9,** 149-180.

Gavalas, A., and Krumlauf, R. (2000). Retinoid signalling and hindbrain patterning. *Curr*. *Opin*. *Genet*. *Dev*. **10,** 380-386.

Gilbert, S. F. (1997). "Developmental Biology." Sinauer Associates, Sunderland, Mass.

Gillespie, D. T. (1977). Exact Stochastic Simulation of Coupled Chemical Reactions. *Journal of Physical Chemistry* **81,** 2340-2361.

Green, N. C., Rambaldi, I., Teakles, J., and Featherstone, M. S. (1998). A conserved C-terminal domain in PBX increases DNA binding by the PBX homeodomain and is not a primary site of contact for the YPWM motif of HOXA1. *J*. *Biol*. *Chem*. **273,** 13273-9.

Guthrie, S., and Lumsden, A. (1991). Formation and regeneration of rhombomere boundaries in the developing chick hindbrain. *Development* **112,** 221-9.

Hamburger, V., and Hamilton, H. (1951). A series of normal stages in the development of the chick embryo. *J*. *Morph*. **88,** 49-92.

Hill, A. V. (1910). Possible effects of the aggregation of the molecules of haemoglobin on its dissociation curves. *J*. *Physiol*. **40,** iv-viii.

Homma, T. a. S., A. (1996). Importance measures in global sensitivity analysis of nonlinear models. *Reliability Engineering and System Safety* **52,** 1-17.

Kalter, H., and Warkany, J. (1959). Experimental production of congenital malformations in mammals by metabolic procedure. *Physiology Review* **39,** 69-115.

Kastner, J. C., Solomon, J. E., and Fraser, S. E. (2002). Modeling a Hox Gene network *in silico* using a Stochastic Simlulation Algorithm. *Developmental Biology* **246,** 122-131.

Langston, A. W., and Gudas, L. J. (1992). Identification of a retinoic acid responsive enhancer 3' of the murine homeobox gene Hox-1.6. *Mech*. *Dev*. **38,** 217-27.

Lauffenburger, D. A., and Linderman, J. J. (1993). "Receptors." Oxford University Press, Oxford.

Leid, M., Kastner, P., and Chambon, P. (1992a). Multiplicity generates diversity in the Retinoic Acid signaling pathways. *Trends in Biochemical Sciences* **17,** 427-433.

Leid, M., Kastner, P., R., L., Nakshatri, H., Saunders, M., Zacharewski, T., Chen, J. Y., Staub, A., Garnier, J. M., Mader, S., and Chambon, P. (1992b). Purification, cloning, and RXR identity of the HeLa-cell factor with which RAR or TR heterodimers to bind target sequences efficiently. *Cell* **68,** 377-395.

Lufkin, T. (1997). Transcriptional regulation of vertebrate Hox genes during embryogenesis. *Crit*. *Rev*. *Eukaryot*. *Gene*. *Expr*. **7,** 195-213.

Lumsden, A., and Krumlauf, R. (1996). Patterning the vertebrate neuraxis. *Science* **274,** 1109-15.

Maconochie, M., Nonchev, S., Morrison, A., and Krumlauf, R. (1996). Paralogous Hox genes: function and regulation. *Annu*. *Rev*. *Genet*. **30,** 529-56.

Maconochie, M. K., Nonchev, S., Studer, M., Chan, S. K., Popperl, H., Sham, M. H., Mann, R. S., and Krumlauf, R. (1997). Cross-regulation in the mouse HoxB complex: the expression of Hoxb2 in rhombomere 4 is regulated by Hoxb1. *Genes Dev*. **11,** 1885-95.

Maden, M. (1999). Heads or tails? Retinoic acid will decide. *Bioessays* **21,** 809-12.

Mader, S., Chen, J. Y., Chen, Z., White, J., Chambon, P., and Gronemeyer, H. (1993). The patterns of binding of RAR, RXR and TR homo- and heterodimers to direct

repeats are dictated by the binding specificites of the DNA binding domains. *Embo. J.* **12,** 5029-41.

Marshall, H., Studer, M., Popperl, H., Aparicio, S., Kuroiwa, A., Brenner, S., and Krumlauf, R. (1994). A conserved retinoic acid response element required for early expression of the homeobox gene Hoxb-1. *Nature* **370,** 567-71.

McGinnis, W., Garber, R. L., Wirz, J., Kuroiwa, A., and Gehring, W. J. (1984). A Homologous Protein-Coding Sequence in *Drosophila* Homeotic Genes and Its Conservation in Other Metazoans. *Cell* **37,** 403-408.

McGinnis, W., and Krumlauf, R. (1992). Homeobox genes and axial patterning. *Cell* **68,** 283-302.

Murphy, P., and Hill, R. E. (1991). Expression of the mouse labial-like homeobox-containing genes, Hox 2.9 and Hox 1.6, during segmentation of the hindbrain. *Development* **111,** 61-74.

Neuteboom, S. T., and Murre, C. (1997). Pbx raises the DNA binding specificity but not the selectivity of antennapedia Hox proteins. *Mol. Cell. Biol.* **17,** 4696-706.

Niederreither, K., Subbarayan, V., Dolle, P., and Chambon, P. (1999). Embryonic retinoic acid synthesis is essential for early mouse post-implantation development. *Nat. Genet.* **21,** 444-8.

Nonchev, S., Maconochie, M., Vesque, C., Aparicio, S., Ariza-McNaughton, L., Manzanares, M., Maruthainar, K., Kuroiwa, A., Brenner, S., Charnay, P., and Krumlauf, R. (1996a). The conserved role of Krox-20 in directing Hox gene expression during vertebrate hindbrain segmentation. *Proc Natl Acad Sci U S A* **93,** 9339-45.

Nonchev, S., Vesque, C., Maconochie, M., Seitanidou, T., Ariza-McNaughton, L., Frain, M., Marshall, H., Sham, M. H., Krumlauf, R., and Charnay, P. (1996b). Segmental expression of Hoxa-2 in the hindbrain is directly regulated by Krox-20. *Development* **122,** 543-54.

Pellerin, I., Schnabel, C., Catron, K. M., and Abate, C. (1994). Hox proteins have different affinities for a consensus DNA site that correlate with the positions of their genes on the hox cluster. *Mol. Cell. Biol.* **14,** 4532-45.

Petkovich, M., Brand, N. J., Krust, A., and Chambon, P. (1987). A human retinoic acid receptor which belongs to the family of nuclear receptors. *Nature* **330,** 444-450.

Phelan, M. L., Rambaldi, I., and Featherstone, M. S. (1995). Cooperative interactions between HOX and PBX proteins mediated by a conserved peptide motif. *Mol Cell Biol* **15,** 3989-97.

Popperl, H., Bienz, M., Studer, M., Chan, S. K., Aparicio, S., Brenner, S., Mann, R. S., and Krumlauf, R. (1995). Segmental expression of Hoxb-1 is controlled by a highly conserved autoregulatory loop dependent upon exd/pbx. *Cell* **81,** 1031-42.

Ronshaugen, M., McGinnis, N. and McGinnis, W. (2002). Hox protein mutation and macroevolution of the insect body plan. *Nature*.

Rorsman, P., Eliasson, L., Renström, E., Gromada, J., Barg, S., and Göpel, S. (2000). The Cell Physiology of Biphasic Insulin Secretion. *News Physiol. Sci.* **15,** 72-77.

Schneider-Maunoury, S., Topilko, P., Seitandou, T., Levi, G., Cohen-Tannoudji, M., Pournin, S., Babinet, C., and Charnay, P. (1993). Disruption of Krox-20 results in alteration of rhombomeres 3 and 5 in the developing hindbrain. *Cell* **75,** 1199-214.

Sham, M. H., Vesque, C., Nonchev, S., Marshall, H., Frain, M., Gupta, R. D., Whiting, J., Wilkinson, D., Charnay, P., and Krumlauf, R. (1993). The zinc finger gene Krox20 regulates HoxB2 (Hox2.8) during hindbrain segmentation. *Cell* **72,** 183-96.

Studer, M., Gavalas, A., Marshall, H., Ariza-McNaughton, L., Rijli, F. M., Chambon, P., and Krumlauf, R. (1998). Genetic interactions between Hoxa1 and Hoxb1 reveal new roles in regulation of early hindbrain patterning. *Development* **125,** 1025-36.

Studer, M., Popperl, H., Marshall, H., Kuroiwa, A., and Krumlauf, R. (1994). Role of a conserved retinoic acid response element in rhombomere restriction of Hoxb-1. *Science* **265,** 1728-32.

Swindell, E. C., Thaller, C., Sockanathan, S., Petkovich, M., Jessell, T. M., and Eichele, G. (1999). Complementary domains of retinoic acid production and degradation in the early chick embryo. *Dev*. *Biol*. **216,** 282-96.

Van Allen, M. I., Kalousek, D. K., Chernoff, G. F., Juriloff, D., Harris, M., McGillivray, B. C., Yong, S. L., Langlois, S., MacLeod, P. M., Chitayat, D., Friedman, J. M., Wilson, R. D., McFadden, D., Pantzar, J., Ritchie, S., and Hall, J. G. (1993). Evidence for multi-site closure of the neural tube in humans. *Am*. *J*. *Med*. *Genet*. **47,** 723-743.

Wilkinson, D. G. (1993). Molecular mechanisms of segmental patterning in the vertebrate hindbrain and neural crest. *Bioessays* **15,** 499-505.

Wilkinson, D. G., Bhatt, S., Cook, M., Boncinelli, E., and Krumlauf, R. (1989). Segmental expression of Hox-2 homoeobox-containing genes in the developing mouse hindbrain. *Nature* **341,** 405-409.